Earth Systems Research Center

Institute for the Study of Earth, Oceans, and Space (EOS)

5-16-2016

Analysis of nitrate in the snow and atmosphere at Summit Greenland: Chemistry and Transport

Dorothy L. Fibiger
Brown University

Jack E. Dibb
University of New Hampshire, Durham, jack.dibb@unh.edu

Dexian Chen
Georgia Institute of Technology

Jennie L. Thomas
Sorbonne Universités

John F. Burkhart
University of Oslo

See next page for additional authors

Comments

Recommended Citation

Authors

Dorothy L. Fibiger, Jack E. Dibb, Dexian Chen, Jennie L. Thomas, John F. Burkhart, L. Gregory Huey, and Meredith G. Hastings

Analysis of nitrate in the snow and atmosphere at Summit, Greenland: Chemistry and transport

Dorothy L. Fibiger[1,2], Jack E. Dibb[3], Dexian Chen[4], Jennie L. Thomas[5], John F. Burkhart[6,7], L. Gregory Huey[4], and Meredith G. Hastings[8]

[1]Department of Chemistry, Brown University, Providence, Rhode Island, USA, [2]Now at NOAA/ESRL/CSD, Boulder, Colorado, USA, [3]Earth System Research Center, Institute for the Study of the Earth, Ocean and Space, University of New Hampshire, Durham, New Hampshire, USA, [4]School of Earth and Atmospheric Sciences, Georgia Institute of Technology, Atlanta, Georgia, USA, [5]LATMOS/ISPL, UPMC Univ. Paris 06, Sorbonne Universités, UVSQ, CNRS, Paris, France, [6]Department of Geosciences, University of Oslo, Oslo, Norway, [7]Sierra Nevada Research Institute, University of California, Merced, California, USA, [8]Department of Earth, Environmental and Planetary Sciences and Institute at Brown for Environment and Society, Brown University, Providence, Rhode Island, USA

Abstract As a major sink of atmospheric nitrogen oxides ($NO_x = NO + NO_2$), nitrate (NO_3^-) in polar snow can reflect the long-range transport of NO_x and related species (e.g., peroxyacetyl nitrate). On the other hand, because NO_3^- in snow can be photolyzed, potentially producing gas phase NO_x locally, NO_3^- in snow (and thus, ice) may reflect local processes. Here we investigate the relationship between local atmospheric composition at Summit, Greenland (72°35′N, 38°25′W) and the isotopic composition of NO_3^- to determine the degree to which local processes influence atmospheric and snow NO_3^-. Based on snow and atmospheric observations during May–June 2010 and 2011, we find no connection between the local atmospheric concentrations of a suite of gases (BrO, NO, NO_y, HNO_3, and nitrite (NO_2^-)) and the NO_3^- isotopic composition or concentration in snow. This suggests that (1) the snow NO_3^- at Summit is primarily derived from long-range transport and (2) this NO_3^- is largely preserved in the snow. Additionally, three isotopically distinct NO_3^- sources were found to be contributing to the NO_3^- in the snow at Summit during both 2010 and 2011. Through the complete isotopic composition of NO_3^-, we suggest that these sources are local anthropogenic particulate NO_3^- from station activities ($\delta^{15}N = 16‰$, $\Delta^{17}O = 4‰$, and $\delta^{18}O = 23‰$), NO_3^- formed from midlatitude NO_x ($\delta^{15}N = -10‰$, $\Delta^{17}O = 29‰$, $\delta^{18}O = 78‰$) and a NO_3^- source that is possibly influenced by or derived from stratospheric ozone NO_3^- ($\delta^{15}N = 5‰$, $\Delta^{17}O = 39‰$, $\delta^{18}O = 100‰$).

1. Introduction

Nitrogen oxides ($NO_x = NO + NO_2$) are short-lived radicals that influence the oxidizing capacity of the atmosphere via interactions with ozone (O_3) and hydroxyl radical (OH). Nitrate (NO_3^-), the end product of NO_x oxidation, is an abundant anion in polar snow. Because NO_3^- can be subject to postdepositional processes such as photolysis and/or evaporative loss [e.g., *Honrath et al.*, 1999; *Rothlisberger et al.*, 2000], NO_3^- in snow can reflect a combination of distant sources and chemistry, as well as local processing and therefore local chemistry. As a result, it can be unclear to what extent NO_3^- that is ultimately archived in ice cores reflects local postdepositional processing and/or loss versus that which is representative of regional scale atmospheric chemistry.

The dominant fraction of oxidized nitrogen ($NO_y = NO_x + HNO_3 + HONO + PAN + $, etc.) transported to Summit is peroxyacetyl nitrate (PAN) [*Kramer et al.*, 2015]. While the amount of PAN transported to Summit decreases in the summer, it remains the dominant species year-round due to formation of PAN in source regions and its long lifetime. PAN can be thermally decomposed to NO_x at any point during its transport, but conditions at Summit are nearly always too cold for this to be a significant contributor to local NO_x [*Kramer et al.*, 2015]. It is, therefore, thought that a main source of NO_x in the lower atmosphere above central Greenland is a photochemical release from snowpack NO_3^- [*Honrath et al.*, 1999; *Thomas et al.*, 2012b, 2011].

A number of studies have investigated the degree to which NO_3^- is lost from the snow upon photolysis (Figure 1, arrows a and b), with the primary reaction pathways
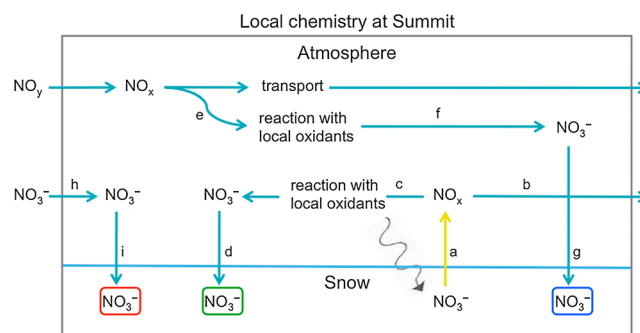
$$NO_3^- + h\nu(+ H^+) \rightarrow NO_2 + OH \tag{R1}$$

$$NO_3^- + h\nu \rightarrow NO_2^- + O(^3P) \tag{R2}$$

Figure 1. Possible paths for NO_3^- deposition and loss at Summit. NO_3^- can be photolyzed in surface snow (arrow a) releasing NO_x to the atmosphere above, which can be transported away (arrow b) or reacted with local oxidants to regenerate NO_3^- (arrow c). NO_3^- deposited back to the snow via this mechanism (arrow d) will contain an isotopic composition that reflects photolysis and oxidation by local gases. Alternatively or in addition, snow NO_3^- could reflect NO_x transported in from outside of Summit that is locally oxidized (arrows e, f, and g) or could represent long-range transported NO_3^- that is deposited and preserved in the snow (arrows h and i).

While the concentration of NO_3^- provides some information about processing of NO_3^- in the snow, more recent studies have shown that the isotopic composition of nitrate can provide more details. NO_3^- in low snow accumulation areas ($\sim$10 cm yr^{-1} snow accumulation), such as on the East Antarctic Ice Sheet, shows significant mass loss and redistribution such that a strong decrease in NO_3^- concentration is observed with depth [*Blunier et al.*, 2005; *Erbland et al.*, 2013; *Frey et al.*, 2009; *Shi et al.*, 2015]. In these studies, the NO_3^- found below the surface in snowpits is generally highly enriched ($\delta^{15}N > 300$‰) in the heavier isotope of nitrogen ($\delta^{15}N = (^{15}N/^{14}N_{sample})/(^{15}N/^{14}N_{N2 \, in \, air \, (reference)}) - 1 \times 1000$‰),

as a result of preferential loss of NO_3^- with greater ^{14}N. Based upon theoretical and laboratory-based predictions of the fractionation factor associated with photolysis of NO_3^- (e.g., -40 to -74‰ [*Berhanu et al.*, 2014; *Frey et al.*, 2009]), the highly enriched values observed in East Antarctica are explained by significant photolytic loss of NO_3^- from the snowpack [*Erbland et al.*, 2013].

In contrast, at Summit, Greenland ($\sim$65 cm yr^{-1} snow accumulation), the NO_3^- in the snow is largely preserved. *Hastings et al.* [2004] found little changes in the isotopes of NO_3^- in snow sampled on the surface in March and resampled in snowpits at 33 cm depth in August. Recently, *Fibiger et al.* [2013] found a strong, linear relationship between the oxygen isotopes of NO_3^- ($\delta^xO = (^xO/^{16}O_{sample})/(^xO/^{16}O_{VSMOW}) - 1 \times 1000$‰, where $x = 18$ or 17; $\Delta^{17}O = \delta^{17}O - 0.52 \times \delta^{18}O$). With the current understanding of photolysis of nitrate in snow, the associated isotopic fractionation for $\Delta^{17}O$ and $\delta^{18}O$ in NO_3^- remaining in the snow, and possible exchange of oxygen atoms in the snow, this relationship could not be explained in the presence of significant postdepositional loss or processing of NO_3^- [*Fibiger et al.*, 2013].

Based on snow NO_3^- data from both 2010 and 2011, the relationship found between $\delta^{18}O$ and $\Delta^{17}O$ indicates that NO_3^- in the snow at Summit is influenced, primarily, by two oxidants of differing isotopic composition. From the linear relationship ($\Delta^{17}O = 0.46 \times \delta^{18}O - 6.9$, $R^2 = 0.9$), the high end-member ($\delta^{18}O = 100$‰ and $\Delta^{17}O = 39$‰) is similar to that expected for ozone, while the low end-member ($\delta^{18}O = 15$‰ and $\Delta^{17}O = 0$‰) is closest in isotopic composition to diatomic oxygen. In the absence of significant NO_3^- loss from the snow, $\delta^{15}N$-NO_3^- in snow and ice at Summit may reflect NO_x sources [*Hastings et al.*, 2009] or some combination of source $\delta^{15}N$ and fractionation with processing (e.g., PAN chemistry) during transport. The $\delta^{18}O$ and $\Delta^{17}O$-NO_3^-, meanwhile reflect the relative abundance of oxidants implicated in the NO_3^- formation pathway [e.g., *Hastings et al.*, 2004; *Morin et al.*, 2008].

While the isotope studies suggest very little loss or redistribution of NO_3^- from the snow at Summit, there are significant NO_x concentrations observed above the snow [*Dibb et al.*, 2002; *Honrath et al.*, 2002; *Yang et al.*, 2002]. The surprisingly high NO_x concentrations, up to 50 pptv measured in the boundary layer, have been ascribed to photolysis of NO_3^- in the snow. Based on modeling of observed concentrations of a suite of gases at Summit, only a 2% loss of NO_3^- from the snow, prior to burial below the photic zone, is required to explain the NO_x concentrations above the snowpack in summertime [*Thomas et al.*, 2011]. This minimal loss fits with isotopic observations of nitrate at Summit thus far. However, recent modeling of the isotopic composition of nitrate under conditions of postdepositional photolytic loss at Dome C on the East Antarctic ice sheet [*Erbland et al.*, 2015] suggests that a significant amount of recycling of NO_3^- can take place locally (Figure 1, arrows a, c, and d)—i.e., NO_3^- is photolyzed and NO_x escapes the snow, this NO_x reacts in the gas phase above the snow and is either transported away (Figure 1, arrow b) or redeposited locally as NO_3^- (Figure 1, arrows c and d). If this process was important at Summit as well, the $\delta^{15}N$ of NO_3^- in the snow should reflect both

photolytic loss and redeposition, while we would expect the $\delta^{18}O$ and $\Delta^{17}O$ of NO_3^- in the snow to reflect the local oxidant composition and any fractionation with redeposition.

The photolytic processing of NO_3^- can also include reactions of the photolytic products which remain in the condensed phase. NO_3^- can be photolyzed to NO_2^-, which will be converted back to NO_3^- in the snow. These reactions will alter the oxygen isotopic composition of the snow NO_3^-, without altering the $\delta^{15}N$. The change in $\delta^{18}O$ and $\Delta^{17}O$ depends on the isotopic composition of the water that makes up the snow [*McCabe et al.*, 2005]. This oxygen exchange happens simultaneously with nitrate photolytic loss from the snowpack, and therefore, both isotopic effects are expected.

If the NO_3^- in the snow is the result of NO_x that is transported in from outside of Summit and then converted to NO_3^- and deposited (Figure 1, arrows e, f, and g), then the $\delta^{15}N$ should reflect long-range transport of NO_x or NO_y to Summit as a result of midlatitude NO_x emission sources, while the oxygen isotopic composition is expected to reflect local oxidizing conditions. For instance, in the presence of sunlight, any NO_2 lost from the snow as a result of photlysis will cycle rapidly with NO, erasing the original oxygen isotopic content of the NO.

$$NO_2 + hv \rightarrow NO + O(^3P) \tag{R3}$$

$$NO + O_3 \rightarrow NO_2 + O_2 \tag{R4}$$

Eventually, the NO_2, which now reflects the isotopic composition of local O_3, will be further oxidized to HNO_3.

$$NO_2 + OH \rightarrow HNO_3 \tag{R5}$$

In this case, the isotopic composition of HNO_3 will be two thirds derived from O_3 and one third from OH. The isotopic composition of OH is currently not well constrained, but it is assumed to be in isotopic equilibrium with water vapor, depending on local conditions [*Morin et al.*, 2007]. Calculated for average summertime conditions at Summit, the OH should contain greater than 98% the isotopic composition of water. This will result in a $\Delta^{17}O$ not significantly different than that of H_2O vapor (~0‰) and a $\delta^{18}O$ that either directly reflects that of H_2O vapor (~ −10‰) or includes fractionation. The most current estimate of the fractionation of OH in equilibrium with water is ~ −40‰ [*Michalski et al.*, 2012], and in this case, OH at Summit would be expected to have a $\delta^{18}O$ of ~ −50‰. The isotopic composition of O_3 is unique among oxidants, with typical $\Delta^{17}O$ of ~26‰ and $\delta^{18}O$ of ~115‰ [*Vicars and Savarino*, 2014]. As demonstrated by *Vicars and Savarino* [2014, and references therein], these values reflect the properties of bulk O_3, while the reactions that produce NO_3^- interact with the terminal oxygen atoms of O_3, such that the isotopic composition transferred to NO_3^- is ~40‰ for $\Delta^{17}O$ and ~128‰ for $\delta^{18}O$. These isotopic values reflect tropospheric O_3, while stratospheric O_3 values have been observed to be higher, close to 35‰ for bulk $\Delta^{17}O$ (53‰ for terminal $\Delta^{17}O$) [*Krankowsky et al.*, 2007].

Attempts to model the oxygen isotopic composition of NO_3^- at Summit, Greenland, generally underestimate the $\Delta^{17}O$-NO_3^- observed in spring and summer due to the expected dominance of (R5) [*Alexander et al.*, 2009; *Kunasek et al.*, 2008]. Both *Alexander et al.* [2009] and *Kunasek et al.* [2008] posited that local halogen chemistry could account for this difference. In particular, the spring BrO concentrations of up to 5.5 pptv [*Liao et al.*, 2011b] at Summit could be high enough to increase the simulated $\Delta^{17}O$-NO_3^- to better match observations. BrO imparts a high $\delta^{18}O$ and $\Delta^{17}O$ on to NO_3^- because its oxygen originates from O_3, as follows:

$$Br + O_3 \rightarrow BrO + O_2 \tag{R6}$$

$$BrO + NO \rightarrow NO_2 + Br \tag{R7}$$

$$NO_2 + BrO + M \rightarrow BrONO_2 + M \tag{R8}$$

$$BrONO_2 + H_2O \rightarrow HNO_3 + HOBr \tag{R9}$$

The resulting HNO_3 in (R9) would have a much higher $\delta^{18}O$ and $\Delta^{17}O$-NO_3^- than that formed in (R5) because of the greater influence of O_3 [e.g., *Morin et al.*, 2012, and references therein]. The higher than predicted snow NO_3^- oxygen isotopic values would then be explained as a result of the local recycling of photolysis-derived NO_x and redeposition of NO_3^- (Figure 1, arrows a, c, and d) [*Alexander et al.*, 2009; *Kunasek et al.*, 2008]. *Jarvis et al.* [2009] also suggested that local recycling of NO_3^- (Figure 1, arrows a, c, and d) at Summit may influence the NO_3^- in the snow, based on an observed offset in $\delta^{18}O$-NO_3^- in the snow and air, despite similar $\delta^{15}N$-NO_3^- in snow NO_3^- and HNO_3 captured from the air (via mist chamber). *Fibiger et al.* [2013], however,

found that postdepositional loss and/or recycling are not prominent processes at Summit during spring and early summer. The NO_3^- in snow, rather, is interpreted as a direct, atmospheric signal, which is representative of long-range transport (Figure 1, arrows h and i). We investigate these contrasting findings by examining whether there are direct connections between atmospheric composition and the concentration and isotopic composition of NO_3^- in surface snow and the atmosphere at Summit.

2. Methods

2.1. Snow Concentration and Isotope Measurements

Two 5 week field seasons were conducted in late spring at Summit, Greenland: 17 May to 22 June 2010 and 24 May to 26 June 2011. Throughout both seasons, surface snow samples comprising the dominant stratigraphic layer, as described in *Dibb et al.* [2007], were collected at 4 or 12 h intervals. This surface layer typically ranged from 0.5 to 3.0 cm in depth and 100 to 400 cm^2. All snow samples were collected within a 2×10 m area in the clean air sector (approximately 1.0 km to the south of the station). This area is generally upwind of the station, though there are periods of "north winds" during each field season when air passes over the station before the sampling area or the winds are low enough that there may be station influence on the snow. North wind conditions are defined as wind between 342 and 72° or less than 2 m s^{-1}. During these events, camp activities that may pollute the snow are limited as much as possible, though the generator is run continuously. At each time point three adjacent samples of 100–400 cm^2 were collected. (The mass of each sample is reported with the data set at ACADIS, see Acknowledgments below.) Every tenth bottle, a blank was collected, which was handled identically to the samples, with approximately 10 mL of 18 MΩ water added in place of the snow. Samples were stored frozen in high-density polyethylene (HDPE) bottles until analysis in laboratories at University of New Hampshire (UNH) and Brown University. Snow samples were first analyzed on a Dionex ion chromatograph (IC) for a suite of ion concentrations, including chloride (Cl^-), bromide (Br^-), sulfate (SO_4^{2-}), NO_3^-, sodium (Na^+), ammonium (NH_4^+), potassium (K^+), magnesium (Mg^{2+}), and calcium (Ca^{2+}). Immediately upon melting in the UNH lab, aliquots where taken for the IC analysis, and the remainder was refrozen for subsequent transfer to Brown. The analysis and QA/QC followed protocols described in *Dibb et al.* [2007] and yielded an uncertainty of 10%.

The NO_3^- was analyzed for the complete isotopic composition ($\delta^{15}N$, $\delta^{18}O$, $\Delta^{17}O$) at Brown University. The isotopes were determined using the bacterial denitrifier method, explained in detail in *Casciotti et al.* [2002], *Sigman et al.* [2001], and *Kaiser et al.* [2007]. In short, denitrifying bacteria that lack the N_2O reductase enzyme quantitatively convert NO_3^- (and NO_2^-) in solution to gaseous N_2O. Using helium as a carrier gas, the analyte N_2O is then measured on a Thermo-Finnegan Delta Plus isotope ratio mass spectrometer at m/z 44, 45, and 46 to determine $\delta^{15}N$ and $\delta^{18}O$ of NO_3^-. Isotopic reference materials, USGS34, USGS35, and IAEA-N3 were prepared in 18.2 MΩ water and analyzed in each set via the same analytical process as samples, and the samples are corrected to a linear fit of the standard values [*Kaiser et al.*, 2007]. (Note that USGS35 is not used as a standard for $\delta^{15}N$.) For the $\delta^{15}N/\delta^{18}O$ analysis, all samples and standards were injected so the amount of NO_3^- was 10 nmol. For determination of $\Delta^{17}O$-NO_3^- ($\Delta^{17}O = \delta^{17}O - 0.52 \times \delta^{18}O$), the N_2O was passed through a gold tube heated to 770°C, resulting in N_2 and O_2 [*Kaiser et al.*, 2007]. The O_2 is then measured at m/z 32, 33, and 34 and corrected based upon linearly fitting reference materials USGS35 and USGS34 to known values. All $\Delta^{17}O$ analysis was done on 50 nmol of NO_3^-. The reference material values and reproducibility for each isotopic quantity are detailed in Table 1.

To calculate the isotopic composition of NO_3^- for each snow-sampling event, a weighted average of the values for the triplicate samples was taken. For example:

$$\delta^{18}O - NO_3^- = \frac{[NO_3^-]_1(H_2Omass)_1\delta^{18}O_1 + [NO_3^-]_2(H_2Omass)_2\delta^{18}O_2 + [NO_3^-]_3(H_2Omass)_3\delta^{18}O_3}{[NO_3^-]_1(H_2Omass)_1 + [NO_3^-]_2(H_2Omass)_2 + [NO_3^-]_3(H_2Omass)_3} \quad (1)$$

where H_2Omass is the mass of snow collected and the same process used for $\delta^{15}N$ and $\Delta^{17}O$.

2.2. Atmospheric Concentration and Isotope Measurements

Atmospheric gas phase soluble ion concentrations (Br^-, nitrite (NO_2^-), NO_3^-) were measured in 0.5 h intervals using a mist-chamber (MC) system coupled to a Dionex IC. The automated two-channel sampling and analysis system has been described previously [*Dibb et al.*, 2010]. In previous studies independent inlets were

Table 1. Error Statistics for Isotopic Standards and Snow Sample Replicates

	$\delta^{18}O$, $1\sigma_p$ (‰)[a]	$\delta^{18}O$, n[b]	$\delta^{18}O$ Standard Value (‰)[c]	$\Delta^{17}O$, $1\sigma_p$ (‰)[a]	$\Delta^{17}O$, n[b]	$\Delta^{17}O$ Standard Value (‰)[c]	$\delta^{15}N$, $1\sigma_p$ (‰)[a]	$\delta^{15}N$ Standard Value (‰)[c]
IAEA-N3	0.37	160	25.6	--	--	--	0.02	4.7
USGS34	0.79	158	−27.9	0.48	246	−0.292	0.02	−1.8
USGS35	0.46	160	57.5	0.72	241	21.6	--	--
Sample replicates	0.7	271	--	0.9	271	--	0.2	--

[a]$\sigma_p = \sqrt{\sum_{i=1}^{k}(n_i - 1)s_i^2 / \sum_{i=1}^{k}(n_i - 1)}$, where n_i and s_i^2 are the size and variance of the ith set of samples, respectively, and k is the total number of sample sets.
[b]n is the number of standards or sample replicates (n is the same for $\delta^{18}O$ and $\delta^{15}N$).
[c]$\delta^{18}O$ standard values from *Böhlke et al.* [2003] and $\Delta^{17}O$ standard values recalculated from *Böhlke et al.* [2003] using the linear $\Delta^{17}O$ ($\Delta^{17}O = \delta^{17}O - 0.52 \times \delta^{18}O$).

used for each channel to assess gradients (with height above the snow, or between firn air and the atmosphere). In this study a single inlet fitted with a Millipore 90 mm Fluoropore PTFE 1 μM pore size filter to remove particulates was employed to sample air approximately 1 m above the snow throughout the field season, resulting in paired samples in 2010. Particulate NO_3^- is a very small fraction of NO_3^- found in Greenland; only about 3% of total atmospheric NO_3^- at Summit is in the aerosol phase [*Dibb et al.*, 1994; *Jaffrezo and Davidson*, 1993; *Silvente and Legrand*, 1995]. Therefore, the mist chamber HNO_3 is expected to be representative of NO_3^- in the atmosphere at Summit. The filter was changed every 2–3 days or when blocked by snow. In 2011, a third MC was added to increase the volume of air sampled during each sampling interval, and hence the mass of NO_3^- collected, to facilitate the isotopic measurements. The atmospheric sampling was located ~200 m from the snow sampling.

At the end of each sampling interval 5 ml of the ultrapure water in one of the samplers was injected into the IC. For NO_2^-, Br^-, and NO_3^-, there is a detection limit of 0.5 pptv and uncertainty of 15%. Any sample solution remaining in that MC was transferred into an amber HDPE bottle. The entire samples in the second (2010 and 2011) and third (2011) MCs were transferred to separate HDPE bottles. The collection bottles for isotope analysis were changed every 12 h and then frozen for shipment to the laboratory at Brown for analysis of $\delta^{15}N$ and $\delta^{18}O$ of NO_3^-.

In these MC samples, [NO_3^-] was low enough that they could not be analyzed directly via the bacterial denitrifier method. The samples were concentrated by anion exchange resin, which has been used previously by several groups [*Erbland et al.*, 2013; *Frey et al.*, 2009; *Silva et al.*, 2000]. A 0.3 cm^3 Bio-Rad AG 1-X8 200–400 mesh chloride form ion exchange resin was used to capture NO_3^- from the sample; the NO_3^- was then eluted from the resin with 10 mL of 1 M NaCl solution. The NaCl always has a small, but significant, NO_3^- blank or NO_3^- impurity associated with it. Within a single batch of NaCl (Fisher brand) the NO_3^- had a constant concentration and isotopic composition. For the NaCl used with samples here, different bottles were found to have a range of 0.5–1 μM NO_3^- in 1 M NaCl solution (determined colorimetrically by a Westco Scientific SmartChem 200 discrete chemistry analyzer). The $\delta^{15}N$ of the NaCl ranged from −2.7 to +0.6‰ and the $\delta^{18}O$ from 13.4 to 30.6‰, depending on the batch of NaCl used. To eliminate the influence of the NO_3^- impurity on sample isotope measurements, 18.2 MΩ water of a similar volume to the samples was put through the same conditions as samples with each sample set. The resultant concentration and isotopic values were corrected out of the sample and reference materials. This is important, even in higher concentration samples, if the isotopic value of NO_3^- in NaCl is significantly different from that of the material being analyzed. Additionally, there is some fractionation associated with the concentrating method, so 0.1 μM standards USGS34, USGS35, and IAEA-N3, were put through the concentration method with each analytical set. Thus, a three-step correction was required: first, all concentrated samples, concentrated standard materials, and NaCl impurity "blanks" were linearly corrected to typical USGS34, USGS35, and IAEA-N3 that are analyzed with every sample set to account for the denitrifier method and mass spectrometry uncertainties [*Kaiser et al.*, 2007]; second, the NO_3^- contained in the NaCl solution was subtracted out by mass balance to remove the influence of this impurity; finally, the samples were corrected based on linear fitting to the known reference material values (USGS34, USGS35) that had been run through the concentration method. In general, the additional corrections (second and third) resulted in a 2–3‰ change in the $\delta^{15}N$, with a maximum change of 5‰ and a 5–15‰ change in $\delta^{18}O$ of the standards, with a maximum change of 25‰. The NO_3^- impurities accounted for the vast majority of this additional correction and the positive $\delta^{18}O$ of NO_3^- in the NaCl accounts for the large range in $\delta^{18}O$ corrections. Despite the use of the concentrating method,

there were times when several samples had to be combined for the 10 nmol of NO_3^- required for analysis. This caused variable time resolution (12–48 h, sometimes discontinuous) and eliminated most of the duplicate samples at any time point. Additionally, there was insufficient NO_3^- in the atmospheric samples for analysis of $\Delta^{17}O$.

BrO was measured by Chemical Ionization Mass spectrometry (CIMS). The configuration of the CIMS has been described by *Liao et al.* [2011b]. The primary reagent ion was $I^- \cdot H_2O$. BrO was ionized inside the CIMS and measured as $BrO \cdot I^-$ [*Neuman et al.*, 2010].

$$BrO + I^- \cdot H_2O \rightarrow BrO \cdot I^- + H_2O \qquad (R10)$$

Due to the unstable nature of BrO, direct calibration of BrO in the field was unavailable. Br_2 from a permeation tube (Kin-tek) was added periodically into the inlet to track the CIMS sensitivities in the field (R10), while the sensitivities to BrO were obtained in the laboratory by comparing sensitivities to BrO and Br_2 [*Liao et al.*, 2011b]. The emission rate of Br_2 permeation tube was measured in the field by spectroiodometric technique [*Wu et al.*, 1963].

$$Br_2 + I^- \cdot H_2O \rightarrow Br_2 \cdot I^- + H_2O \qquad (R11)$$

During the 2010 campaign, sensitivity to BrO was 5–15 Hz pptv^{-1} and the detection limit was ~1–1.5 pptv based on 1 min averaged data. During the 2011 campaign, sensitivity to BrO was 10–35 Hz pptv^{-1} and the detection limit was <0.3 pptv based on 1 min averaged data. The detection limit was significantly improved during the 2011 campaign, partially due to increased sensitivities with a new detector and ion source. The total uncertainty was ~30% for BrO measurements in both years.

NO and NO_y were measured by the chemiluminescence method described by *Ryerson et al.* [2000]. The instrument has two channels: one channel measured NO directly by chemiluminescence, and the other was equipped with a heated Molybdenum converter which converts all NO_y species into NO, and the product NO was measured to quantify NO_y. During the 2011 campaign, high-frequency noise was observed on both NO and NO_y channels, probably due to a deteriorating photomultiplier; therefore, a low-pass filter with a cutoff of 0.05 Hz was applied to the raw data. During the two campaigns the detection limit was ~1–1.5 pptv, and the total uncertainty was ~10% for both NO and NO_y channels.

2.3. Transport Modeling

We used the Lagrangian FLEXible PARTicle Dispersion Model (FLEXPART) [*Stohl et al.*, 2005] to evaluate (1) the seasonal transport patterns at Summit during our two seasons in 2010 and 2011 and (2) transport events on 22–25 May 2010 and 24–26 June 2011. In both model investigations, FLEXPART was driven using European Center for Medium-range Weather Forecasting model ($0.25° \times 0.25°$ horizontal resolution, 92 vertical levels) global meteorological fields. FLEXPART was run in two ways. First, the model is used to study seasonal transport to Summit during the two campaign years (2010 and 2011 seasons). For this, we calculate the mean transport during 17 May to 22 June 2010 and 24 May to 26 June 2011. Simulations are conducted backward in time, as this provides a more efficient way to calculate a source-receptor relationship when one is interested in a single receptor. The model was configured with 3-hourly releases of 90,000 particles each from a grid box local to Summit. The particles were parameterized as a passive tracer with a 20 day lifetime. This parameterization removes the particles after 20 days and is intended only to provide an air mass history. In this configuration, one may use the FLEXPART model to produce maps of potential emission sensitivity (PES) (in units of s kg^{-1}), which is proportional to the particle residence time in that cell. It is a measure for the simulated mixing ratio at the receptor that a source of unit strength (1 kg s^{-1}) in the respective grid cell would produce. By taking the lowest model layer (<100 m above ground level) one can create a map of residence time or sensitivity to source regions. This provides information on where and when the air mass would be sensitive to surface emissions. When conducting transport simulations over a long period (e.g., several weeks of the campaign), these values must be normalized so that patterns separate from immediate local transport can be seen. We normalized the seasonal average using the long-term mean transport climatology from Summit for the period of January 2000 to December 2011. The resulting data provides seasonal transport anomaly from the long-term mean transport for each season. Second, the model is run for specific events. Separate FLEXPART runs in backward mode were completed for each day with releases (100,000 particles) from 9:00–17:00 UTC in 2010 and 13:00–21:00 UTC in 2011, bracketing the times of largest isotope anomaly. Using the plume-clustering algorithm included in FLEXPART, we are able to map the air mass transport history immediately prior to the observations [*Dorling et al.*, 1992; *Stohl et al.*, 2002].
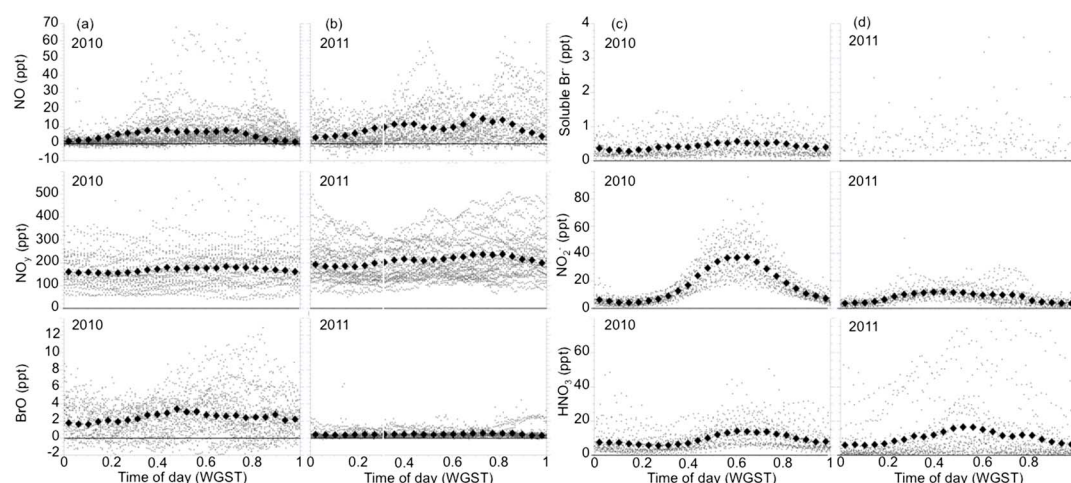
Figure 2. Hourly averages (black diamonds) and all data (grey points) for gas phase NO, NO_y, and BrO in (a) 2010 and (b) 2011. Soluble Br^-, NO_2^- and HNO_3 in (c) 2010 and (d) 2011 in Western Greenland Standard Time (WGST). BrO values are significantly higher in 2010 than 2011, while NO and NO_y have similar average values, but different distributions. Br^- and soluble NO_2^- values are significantly higher in 2010 than 2011, HNO_3 has similar values with a different time distribution. No hourly averages of soluble Br^- are reported in 2011 because there are too few data points above the detection limit.

3. Results

In both the 2010 and 2011 campaigns, the same suite of gas phase and snow measurements was made. Both campaigns showed high variability in both concentration and isotope measurements, which is typical of what has been observed at Summit in the past (detailed below). We first consider the gas phase concentrations of NO, NO_y, BrO, and soluble gases, followed by the snow NO_3^- concentration and isotopes, and, finally, context for our discussion and interpretation based on transport modeling.

3.1. Gas Phase Concentrations

The mixing ratios of reactive nitrogen oxides and active bromine above the snow at Summit were quite different in some regard, between the two field campaigns. Focusing first on compounds that are believed to be dominated by emissions from the snowpack [*Thomas et al.*, 2012a], we note that hourly means (and medians, not shown) of NO were consistently higher by several pptv during summer 2011; this enhancement was largest (>4 pptv) from 17:00 to 23:00 Western Greenland Standard Time (WGST) (Figures 2a and 2b). In contrast, soluble NO_2^- mixing ratios were much higher in 2010, particularly from about 11:00–23:00 WGST (Figures 2c and 2d). Reactive bromine (both BrO and the soluble Br^- measured by MC/IC) was also higher by at least a factor of 5 throughout the day during 2010 (Figure 2). Nitric acid above the snow can be enhanced by long-range transport events, but it has been suggested that local production from NO and HO_x emitted from the snowpack can be the dominant source for much of the summer at Summit [e.g., *Dibb et al.*, 2002; *Dibb and Fahnestock*, 2004; *Thomas et al.*, 2011]. Hourly mean HNO_3 mixing ratios were similar in 2010 and 2011, but we observed several hour offset in the timing of the daily peak (12:00–14:00 WGST in 2011 versus 14:00–18:00 in 2010) and note that the nighttime minimum was not as deep in 2010 (Figures 2c and 2d). The afternoon and evening enhancement of HNO_3 in the 2010 campaign is more pronounced in the hourly medians (not shown). Mixing ratios of NO_y increased just 10–20 pptv from early morning minima to broad afternoon maxima in both seasons, 2011 had higher levels by 20–30 pptv throughout the average daily cycle (Figures 2a and 2b).

The nitrogen oxide species have been measured in a series of Summit campaigns extending back to 1998, but the only previous measurements of reactive bromine were made as part of the Greenland Summit Halogen-HO*x* Experiment (GSHOX) experiment in 2007 and 2008 (summarized in *Thomas et al.* [2012b]). Most of these prior campaigns emphasized the fast photochemistry linking NO_x and HO_x cycles above the snow and focused on model simulations around midday when this chemistry was most active. Comparing our observations during midday to those from GSHOX reveals that NO mean and median mixing ratios were quite low in 2010 (Table 2). Looking further back, the NO means and medians in 2008, 2010, and 2011 were all 1.5–2.5-fold lower than reports for midday during campaigns in 1999, 2000 [*Yang et al.*, 2002], 2003 [*Chen et al.*, 2007], and a

Table 2. Mean (Median) Midday (10:00−15:00 WGST) Gas Phase Mixing Ratios (pptv) During Recent Campaigns at Summit

Species	2011	2010	2008[a]	2007[a]
	5/24 to 6/26	5/17 to 6/22	5/13 to 6/13	6/10 to 7/8
NO	9.8 (8.1)	7.5 (4.6)	11.4 (8.6)	17.2 (12.8)
NO_2^-[b]	11.2 (10.6)	32.5 (30.9)	5.8 (4.7)	7.3 (6.5)
HNO_3	15.5 (8.3)	11.7 (11.0)	11.5 (5.5)	15.9 (12.9)
BrO	0.5 (0.4)	3.0 (2.9)	2.0 (1.5)	2.0 (1.8)
Soluble Br^-[c]	--[d] (--[d])	0.5 (0.3)	0.3 (0.3)	0.7 (0.6)

[a]From *Liao et al.* [2011a] and *Dibb et al.* [2010].
[b]This is strictly soluble nitrite (NO_2^-) as sampled and quantified by the MC/IC system.
[c]See *Liao et al.* [2012] for discussion of soluble bromide.
[d]During the 2011 season bromide was only above detection limits in 211 out of 1406 half-hour mist chamber samples, making summary statistics highly uncertain.

springtime campaign in 2004 [*Grannas et al.*, 2007]. On the other hand, midday soluble NO_2^- in 2010 was more than fourfold higher than during either GSHOX campaign (Table 2). The mean and median soluble NO_2^- mixing ratios reported in 2008, however, were the lowest out of nine campaigns, with the 1999, 2000, 2003, and 2004 results all in the 7–13 pptv range like 2007, and in 1998 the midday mean (median) was 42.7 (42.1) pptv [*Grannas et al.*, 2007]. Midday HNO_3 during our recent campaign varied between the two years, but was within the same range reported for GSHOX (Table 2). During the 1999 and 1998 campaigns midday HNO_3 mean (median) mixing ratios were 16.9 (9.4) and 44.3 (9.4) pptv, respectively [*Grannas et al.*, 2007].

3.2. Snow Nitrate Concentration

In the surface snow, the NO_3^- varied significantly between the 2010 and 2011 seasons sampled at Summit (Figure 3). The [NO_3^-] in the snow ranged from 0.7 to 9.7 μM in 2010, with a mean of 2.8 μM, and in 2011 it ranged from 1.0 to 15.5 μM with a mean of 5.16 μM. This range of [NO_3^-] is similar to that observed in surface snow in May/June 2006 by *Jarvis et al.* [2009] (1 to 6 μM), *Honrath et al.* [2002] (1.2 to 8 μM), and *Hastings et al.* [2004] (0.8 to 5.9 μM).

3.3. Isotope Measurements

The snow $\delta^{18}O$-NO_3^- in 2010 ranges from 37.4 to 93.4‰ with a mean of 78.5‰; while the range is similar in 2011 (28.9 to 93.6‰), the mean of 70.1‰ is significantly different. In contrast, the $\delta^{15}N$-NO_3^- has similar mean values in the two years (−1.3 and −1.4‰) as well as similar ranges (2010: −8.7 to +14.1‰, 2011: −8.2 to +13.4‰). The snow NO_3^- oxygen isotopic composition is similar in range to that observed by *Jarvis et al.* [2009], where they
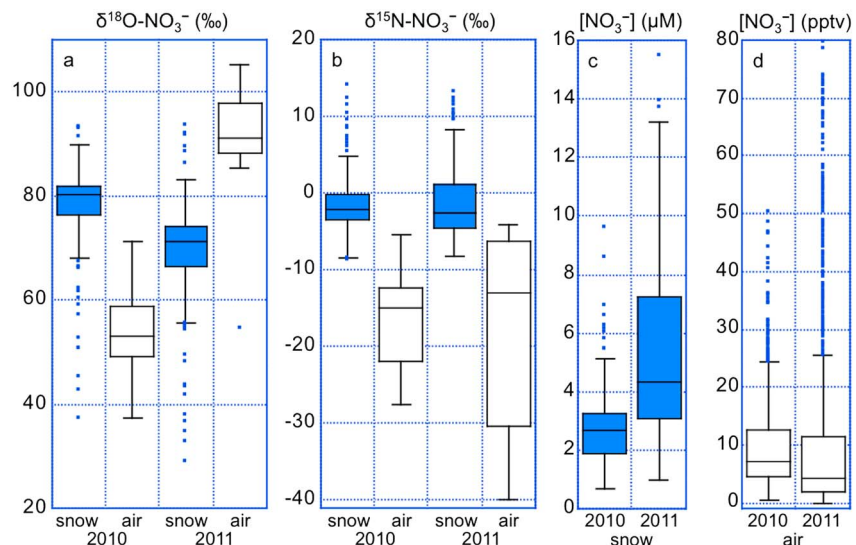

Figure 3. Comparison of snow and air NO_3^- isotopic composition and concentration. Snow (blue) and air (white) from 2010 and 2011 are compared for (a) $\delta^{18}O$ and (b) $\delta^{15}N$. NO_3^- concentration for both years is compared for (c) snow and (d) air. The lines in each diagram show the median value, the boxes show the upper and lower quartiles. The individual points are more than 1.5 times the interquartile distance. Note that the snow NO_3^- concentration and $\delta^{18}O$-NO_3^- above, in addition to the $\Delta^{17}O$-NO_3^- of the same samples, are reported in *Fibiger et al.* [2013].
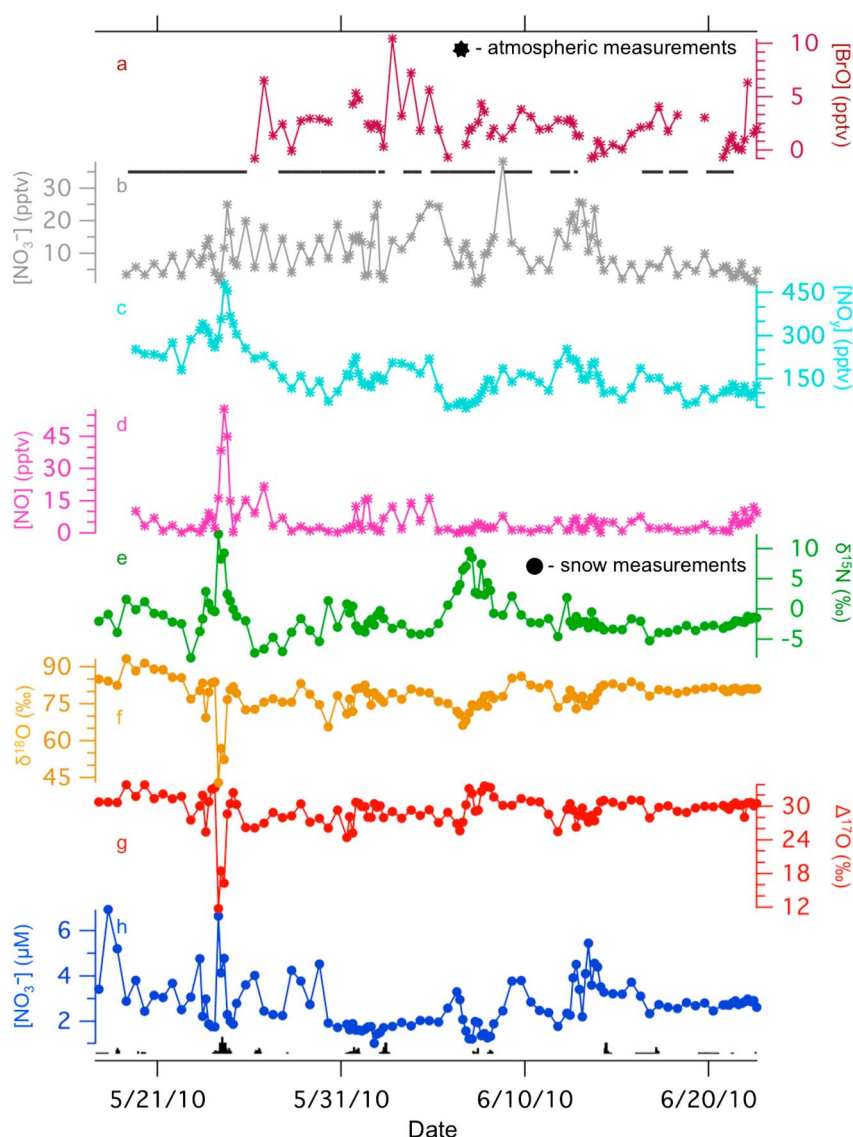
Figure 4. Time series of atmospheric (a–d) and snow (e–h) data for 2010. The atmospheric constituents are on top and marked with stars. The snow measurements are indicated with dots. The black bars at the bottom indicate times Summit Station was under north wind conditions (winds between 342 and 72° or less than $2\,m\,s^{-1}$). The bar length indicates the inverse of the wind speed (longer bars are slower speeds). The dark grey line between Figures 4a and 4b shows the time coverage of the atmospheric NO_3^- isotopic values summarized in Figure 3. All snow samples were collected at 4 or 12 h time intervals in triplicate. The $[NO_3^-]$ is a mean of the triplicates, while the isotopic values are weighted by NO_3^- amount (see section 2.1). The atmospheric observations represent 5 h back averages from the time each snow sample was collected.

found $\delta^{18}O$-NO_3^- from 40 to 110‰. The $\delta^{15}N$-NO_3^- in snow observed by *Jarvis et al.* [2009], however, is lower ($\delta^{15}N$-NO_3^- from −15 to +5‰) than seen in 2010 or 2011.

In contrast to Jarvis, however, the $\delta^{15}N$-NO_3^- in the snow is significantly different from the $\delta^{15}N$-HNO_3 in the air. Both seasons had similar $\delta^{15}N$-HNO_3 in the atmospheric samples, whereas $\delta^{18}O$-HNO_3 was very different between the years. (Figure 3). In 2010, the mean $\delta^{15}N$-HNO_3 in the atmosphere was −16‰, and in 2011, −13‰. The $\delta^{18}O$-HNO_3 was 54‰ in 2010 and 91‰ in 2011. The atmospheric isotopic data, however, represent only 60% of the 2010 field season and 10% of the field season in 2011. In 2010, these data are evenly distributed over the season, while in 2011, all atmospheric data fall during the period of high $[HNO_3]$ from 10 June to 16 June (Figure 5).

In both 2010 and 2011 there is a strong correlation between $\delta^{18}O$ and $\Delta^{17}O$ of NO_3^- in the snow. As shown in *Fibiger et al.* [2013], the relationship of $\Delta^{17}O = 0.46 \times \delta^{18}O - 6.9$ cannot be explained with any significant
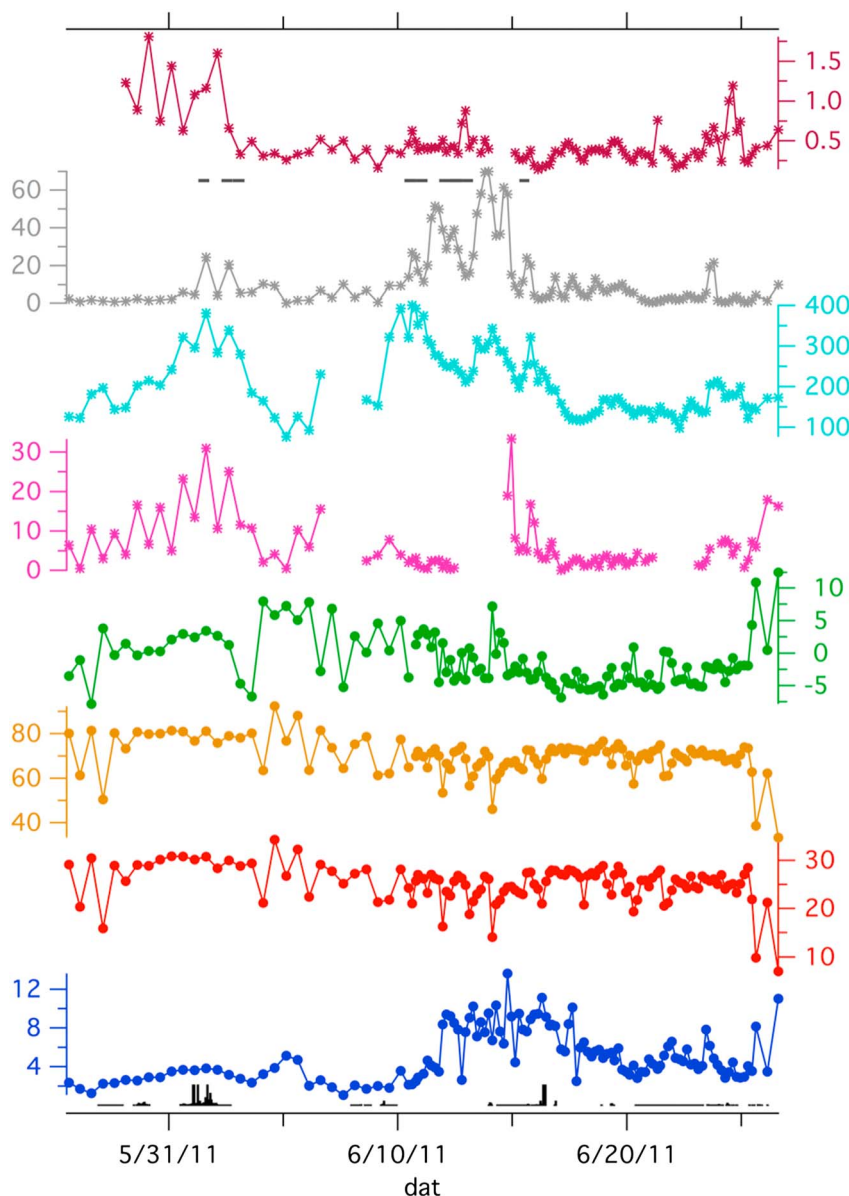
Figure 5. The time series of atmospheric (a–d) and snow (e–h) data for 2011. (a–d) The atmospheric constituents are on top and marked with stars. (e–h) The snow measurements are indicated with dots. The black bars at the bottom indicate times Summit Station was under north wind conditions (winds between 342 and 72° or less than 2 m s^{-1}). The bar length indicates the inverse of the wind speed (longer bars are slower speeds). The dark grey line between Figures 5a and 5b shows the time coverage of the NO$_3^-$ atmospheric isotopic values summarized in Figure 3. All snow samples were collected at 4 or 12 h time intervals in triplicate. The [NO$_3^-$] is a mean of the triplicates, while the isotopic values are weighted by NO$_3^-$ amount (see section 2.1). The atmospheric concentrations represent 5 h back averages from the time each snow sample was collected.

postdepositional processing of NO$_3^-$ in the snow. NO$_3^-$ loss or local recycling of NO$_3^-$ would perturb the linear relationship. Instead, the NO$_3^-$ in the snow is interpreted as a direct atmospheric signal of long-range transported NO$_3^-$. There is no relationship found between any of the isotopes of NO$_3^-$ in the snow and any of the atmospheric constituents measured (Figures 4 and 5). Additionally, in the snow, there is no correlation between δ^{15}N-NO$_3^-$ and the oxygen isotopes of NO$_3^-$. In the atmospheric samples, there is no relationship between δ^{15}N-HNO$_3$ and δ^{18}O-HNO$_3$.

In both seasons, there occur isotope deviations in the NO$_3^-$ in the snow, in which the δ^{18}O and Δ^{17}O both decrease significantly while the δ^{15}N increases (Figure 6). The most obvious event occurs in 2010 on 25 May. In 2011, these excursions bookend the observations: occurring in the first days of sampling (27 and 28 May) and
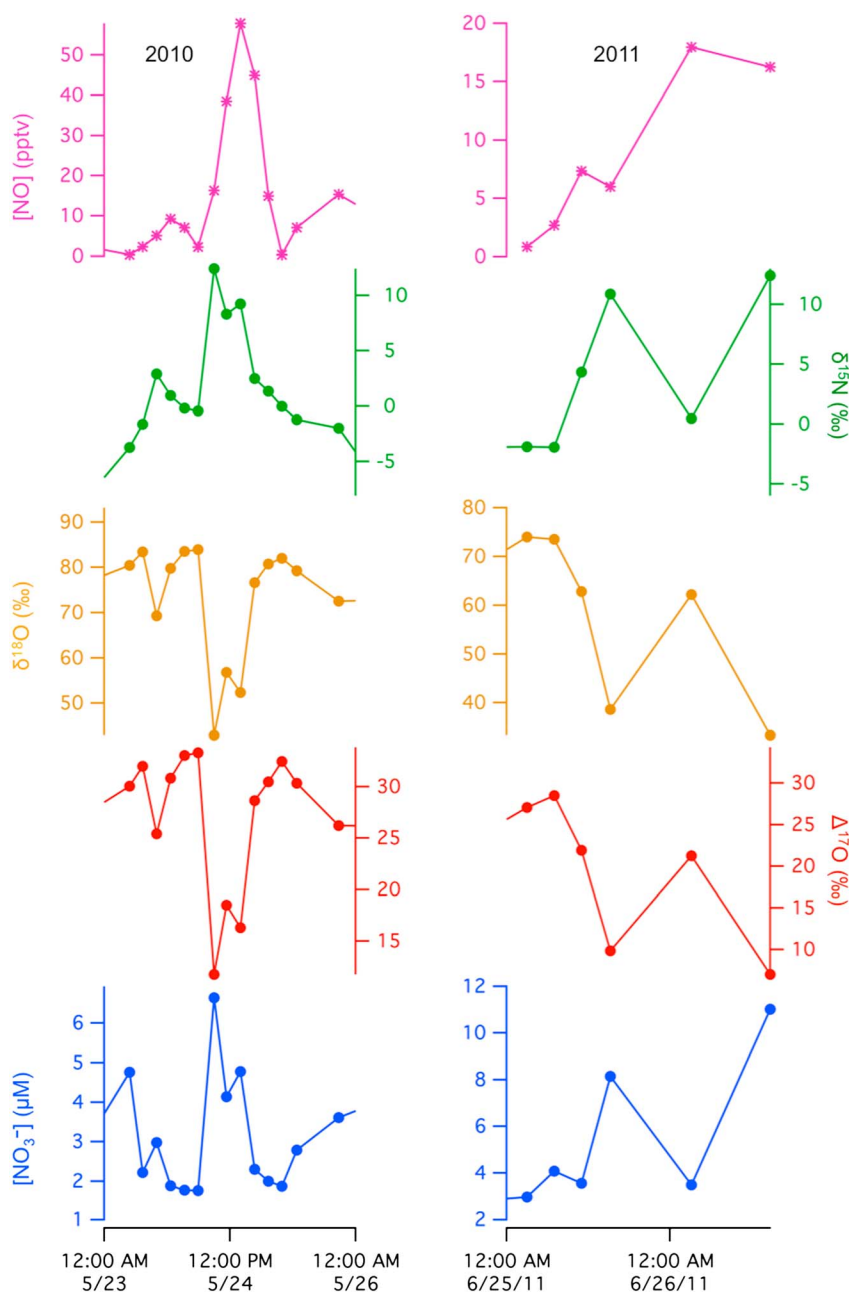
Figure 6. A more detailed look at the NO_3^- isotope and concentration behavior during an isotope deviation in 2010 and one in 2011. Gas phase data is a 5 h back average from the time point of snow collection. Both deviations occur at the same time as the highest NO concentration, indicating the presence of local anthropogenic pollution. Both excursions show a large decrease in $\delta^{18}O$ and $\Delta^{17}O$, with a simultaneous increase in $\delta^{15}N$ and $[NO_3^-]$.

at the very end of the season (26 June). These events do not correspond with any significant changes in atmospheric NO_3^-, BrO, or NO_y. They all, however, happen concurrently with relatively high concentrations of NO, with the 2010 and 26 June 2011 events corresponding with season-high NO concentrations (Figure 6). These unusual NO events seem to be driven by pollution from the camp. Additionally, all the events occur during times when winds are bringing air over camp and then over the sampling area or when the wind speed is less than $0.5\,\mathrm{m\,s^{-1}}$, indicating that NO_3^- pollution from camp may be impacting the samples collected during this time.

3.4. Transport Modeling

Atmospheric transport modeling for each season showed distinct transport patterns and source regions. In 2010 the bulk of air arriving at Summit had a source origin spanning a band from approximately 40°N to
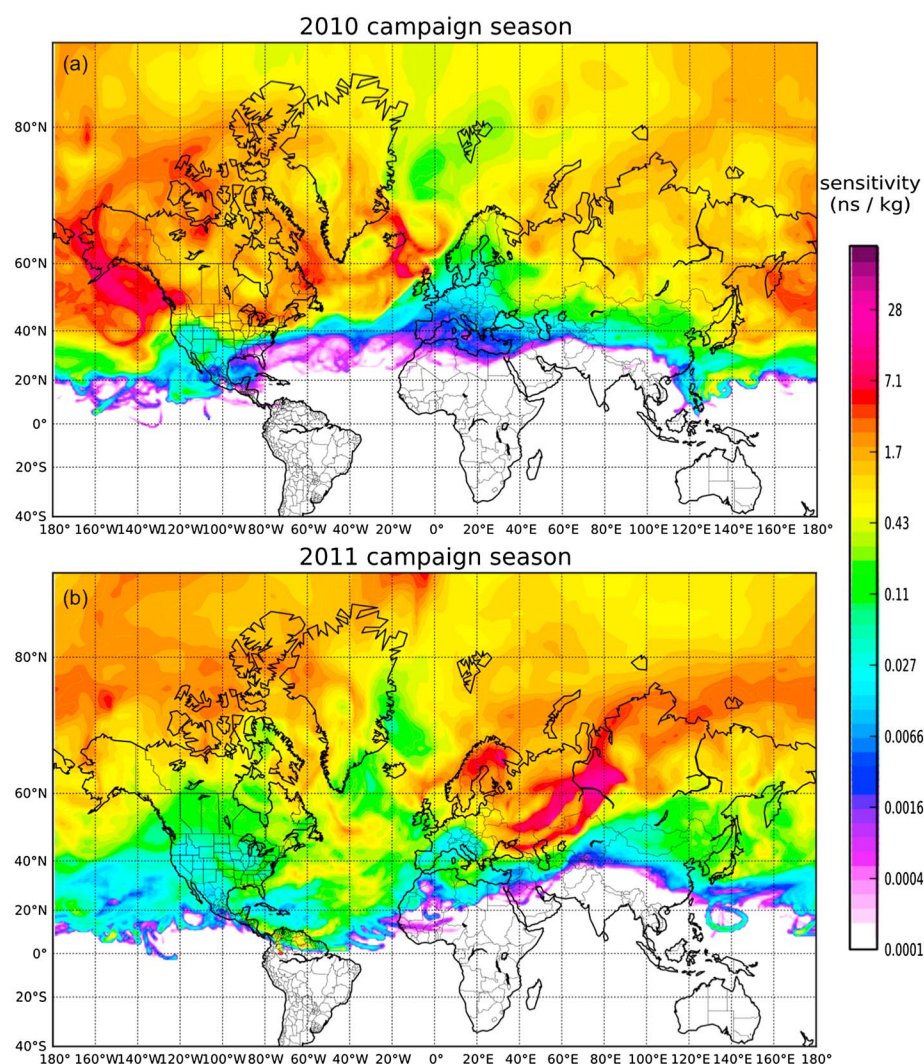
Figure 7. Potential emission sensitivity for transport to Summit, Greenland for (a) 17 May to 22 June 2010 and (b) 24 May to 26 June 2011 as evaluated by the FLEXPART model. The plots show the air mass histories, or residence time, of air in the lowest 100 m of the atmosphere over the period of observation in each of the two seasons. They are normalized by the long-term (2000–2011) mean transport climatologies. It can be seen that during the 2011 season, air was predominately from Eurasia, distinct from the 2010 season which showed typical Westerly transport from North America.

50°N reaching from the western Pacific across central North America and into the North Atlantic. This air mass source region history would indicate preferential sampling of North American emissions, particularly with the strong source region of the North Atlantic, which is a primary transport pathway for emissions leaving the U.S. From a day-by-day analysis (not shown), there were two brief periods early in the season when air masses arrived from Europe, but aside from these episodes transport was distinctly from the west (Figure 7a). This transport pattern is typical of Summit in the early summer period during which sampling took place [*Kahl et al.*, 1997].

During 2011, a more unusual pattern emerges: the source region for air was heavily influenced by Eurasian emissions with a mix of Arctic and North Siberian air masses as well (Figure 7b). The latter two prove to be somewhat episodic but do have an influence on the overall mean climatology. In general, air masses arriving at Summit have a character of both North American and European sensitivity, depending highly on the movement of low-pressure systems south of Greenland as they track across the North Atlantic. Aside from a brief episode from 10 to 13 June (corresponding with the time of higher atmospheric [HNO_3]), air sampled during the campaign was almost entirely from Europe. Leading up to and following the brief incursion of North American air during mid-June 2011, there was a period of stable regional flow from Europe. The latter half of

the campaign period experienced relatively fast transport, heavily dominated from Europe with 20 day potential emission sensitivity (PES) reaching into the center of the continent.

4. Discussion

4.1. Local Chemistry at Summit

Previously, it was thought that local recycling of NO_3^- might be important at Summit [*Jarvis et al.*, 2009; *Kunasek et al.*, 2008]. If this were true, however, there should be some connection between local gas phase concentrations and the isotopes of NO_3^- in the snow. If HNO_3 were formed locally and deposited by cloud-to-ground scavenging of NO_3^- in the snow (Figure 1, arrows d and g), then BrO concentrations above 1 pptv should be influencing NO_3^- in the snow [*Kunasek et al.*, 2008; *Morin et al.*, 2007] via reactions (R6) through (R9). In particular, we expect that when BrO is high, the $\Delta^{17}O$ and $\delta^{18}O$ of nitrate would also be high, as BrO retains the anomalous isotopic signature of the O_3 from which it is derived. The local signal, if important, should be present in the snow as the lifetimes of NO and HNO_3 at Summit are only a few hours. This is evident in the atmospheric HNO_3 and NO concentrations at Summit, as both approach zero at low solar zenith angle. This is evidence that there is some loss or recycling of NO_3^- from the snow in Greenland [*Honrath et al.*, 1999], but as noted above, as little as 2% of NO_3^- loss from the snow can account for observed NO_x concentrations above the snow [*Thomas et al.*, 2011]. This photolysis of NO_3^- to NO_x has a significant influence on local NO_x concentrations and the $\delta^{15}N$-HNO_3 in the atmosphere at Summit, but appears small enough to not have a significant effect on the residual NO_3^- in the snow. If photolysis of NO_3^- to NO_x followed by deposition of locally formed HNO_3 (Figure 1, arrows a, c, and d) was having a strong influence on the NO_3^- in the snow, we would expect that snow NO_3^- concentrations would reflect NO and HNO_3 atmospheric concentrations. There was, however, no connection found between the local concentrations of BrO, NO, or NO_y and any of the isotopes of NO_3^- or [NO_3^-]. This lack of relationship was found using 3, 5, and 12 h back averages of the gas phase data, from each time point that a snow sample was taken, accounting for potential variations in the lifetime of NO_x against deposition as NO_3^-. This indicates that local chemistry, either through recycling of NO_3^- or local conversion of NO_x to NO_3^-, is not influencing the NO_3^- preserved in the snow. This lack of relationship is true both across each season and over shorter timescales within. For instance, in 2010 the highest BrO concentrations were found between 3 and 6 June, but the $\delta^{18}O$ and $\Delta^{17}O$ of NO_3^- in the snow were typical of that found during the field season. Additionally, during that time period the BrO concentration is highly variable and that variation is not reflected in the oxygen isotopic composition of NO_3^- found in the snow at Summit. Finally, as shown by *Fibiger et al.* [2013] photolytic processing of the NO_3^- does not have a significant influence on the oxygen isotopes of NO_3^- observed in the snow at Summit. Taken together, the above all suggest that the NO_3^- found in snow at Summit is not a result of local chemistry and scavenging. Rather, the snow NO_3^- at Summit represents a larger pool of atmospheric NO_3^- that is transported to Summit and deposited.

There are also significant differences in the NO_3^- in the snow and atmosphere at Summit in 2010 and 2011, which can be enlightening on their own. First, it is clear that BrO is not having an influence on NO_3^- formation at Summit. If it were, we would expect the NO_3^- collected in the MC to show a higher $\delta^{18}O$ and $\Delta^{17}O$ when there is more BrO ($\Delta^{17}O$ = 19.5 to 35‰, $\delta^{18}O$ = 60 to 100‰, if it directly reflects O_3, both may be up to 1.5 times higher if only the terminal oxygen transfers in formation of BrO [*Johnston and Thiemens*, 1997; *Vicars et al.*, 2012]). In 2010, the $\delta^{18}O$-NO_3^- in the atmosphere has an average value of 54‰, while in 2011 it is 91‰. In 2011 there is very little BrO in the atmosphere, with concentrations never exceeding 2.0 pptv, and during the time of high atmospheric HNO_3 (when atmospheric isotope measurements were possible), it was around 0.5 pptv. In contrast, in 2010 BrO levels ranged between 0 and 10 pptv and were consistently over 2 pptv. This should have resulted in a high $\delta^{18}O$-HNO_3 in 2010 if local chemistry were playing an important role in HNO_3 formation. The 2010 season, however, had a significantly lower average $\delta^{18}O$-HNO_3 (Figure 3a). Therefore, we conclude that BrO chemistry does not have a significant influence on the formation of local HNO_3 at Summit.

It has been suggested in a number of studies that the relatively high accumulation rate at Summit may prevent postdepositional processing of NO_3^-; however, it does not appear that snowfall rates, alone, dictate the lack of photolytic processing of snow NO_3^-. There was a significant difference in surface height change between the two study periods. In 2010, there was a 14 cm increase in height during the observation time, while during the 2011 study period there was only 3 cm of increased height (from ftp://summitcamp.org/pub/data/GEOSummit/Bales_UCM/Bamboo%20Forest/). The 2010 change would be sufficient to reduce the photolysis of NO_3^- by one

e-folding depth (8–10 cm at Summit [*Galbavy et al.*, 2007], but in 2011, the height change should leave all deposited snow in the most active portion of the photic zone. The two years, however, both show the same δ^{18}O–NO$_3^-$, Δ^{17}O-NO$_3^-$ relationship and the same set of contributing NO$_3^-$ sources (section 4.2, below).

Local photochemistry is not a major driver of the variations in [NO$_3^-$] or isotopes of NO$_3^-$ in the snow, but there are still differences in the measurements of snow at consecutive time points. The driving force for these variations seems to be, primarily, spatial heterogeneity in the snow. The triplicate samples represent only a few tens of centimeters spatial scale, which should be capturing only about 25% of the variation observed over tens of meters [*Dibb and Jaffrezo*, 1997].

4.2. Snow and Atmosphere NO$_3^-$

The relationship between the isotopes and concentrations of NO$_3^-$ in the snow and atmosphere at Summit provide further evidence of the lack of locally formed HNO$_3$ influencing snow NO$_3^-$. The δ^{18}O-NO$_3^-$ in the snow is different from the δ^{18}O-HNO$_3$ in the air and is also significantly different between 2010 and 2011. In fact, in 2010 the δ^{18}O-HNO$_3$ in the air is significantly lower than δ^{18}O-NO$_3^-$in the snow (Figure 3a). In 2011, the relationship is the opposite with δ^{18}O higher in the gas phase than in the snow. In the snow, the [NO$_3^-$] is higher in 2011 than in 2010. In the air, there are higher concentrations achieved in 2011, but the mean concentrations are similar (Figures 3c and 3d). While the atmospheric isotopic samples in 2011 cover a small portion of the season, the snow isotopic values in that period are representative of the season on average.

These interannual differences in air-snow offsets provide further evidence that local gas phase HNO$_3$ is not significantly influencing the NO$_3^-$ in the snow. If the local gas-phase HNO$_3$ were influencing the isotopes in the snow, we would expect the δ^{18}O-NO$_3^-$ in the snow in 2011 to be higher on average than in 2010, as the isotopes of gas phase HNO$_3$ exhibit. The snow, however, shows the opposite pattern with higher δ^{18}O-NO$_3^-$ in 2010 than 2011.

There is a consistent offset between δ^{15}N-NO$_3^-$ in the snow and air at Summit. In both 2010 and 2011 the difference in mean values is 10‰. Due to the resolution of the atmospheric HNO$_3$ isotope measurements, it is not possible to look at the offset at any one point in time. The average offset, however, is markedly different than the only other similar observations [*Jarvis et al.*, 2009], where gas phase HNO$_3$ and snow NO$_3^-$ were found to have similar δ^{15}N of approximately −4‰, similar also to the values found in the snow in 2010 and 2011. The HNO$_3$ in the air, however, is distinctly different between the two studies, with mean δ^{15}N-HNO$_3$ in the air found to be −12.6‰ in 2010 and −17.7‰ in 2011. The offset in δ^{15}N-NO$_3^-$ in the atmosphere and snow could be consistent with photolysis of NO$_3^-$ in the snow (Figure 1, arrow a), such that lower δ^{15}N-NO$_x$ leaves the snow to then form HNO$_3$ locally (Figure 1, arrow c). Given the lack of relationship between the atmosphere and snow concentration and isotopes, however, this process must represent a very small portion of the NO$_3^-$ in the snow.

4.3. NO$_3^-$ Sources to Summit

There is no correlation between δ^{15}N and the oxygen isotopes of snow NO$_3^-$, but plotting them against each other reveals an interesting relationship (Figure 8). The surface snow samples from both 2010 and 2011 fall within a triangle, indicating a mix of three isotopically distinct forms of NO$_3^-$ at Summit. The three sources contribute NO$_3^-$ of distinct isotopic composition: δ^{15}N = 16‰, Δ^{17}O = 4‰, and δ^{18}O = 23‰; δ^{15}N = 5‰, Δ^{17}O = 39‰, and δ^{18}O = 100‰; δ^{15}N = −10‰, Δ^{17}O = 29‰, and δ^{18}O = 78‰. The relative contribution of each NO$_3^-$ source to any snow sample can be quantified by the relative distances from each of the three end-members. While source attribution is difficult due to limited and conflicted studies of δ^{15}N of NO$_x$ from various sources [*Fibiger et al.*, 2014; *Walters et al.*, 2015], we can use the complete isotopic composition of the NO$_3^-$, the interannual variations and transport analysis to develop ideas on potential NO$_3^-$ sources.

4.3.1. Seasonal Transport to Summit

The 2010 and 2011 seasons at Summit show distinct transport patterns and air source regions. In 2010, the air is primarily derived from North America, while in 2011 it is primarily from Eurasia, with particular influence from the Ob River, an area of heavy industrial activity. It is notable that in 2011 there is a short period of time (10–13 June) when the air is transported from North America and the atmospheric [HNO$_3$] during this time is more reflective of "typical" Summit conditions. The very different transport patterns over the two years are reflected in differing isotopic compositions of NO$_3^-$ in the snow across the two years. The interannual isotopic variation may reflect differing isotopic compositions derived from different regional sources, potential fractionations during transport to Summit, or a combination of the two.
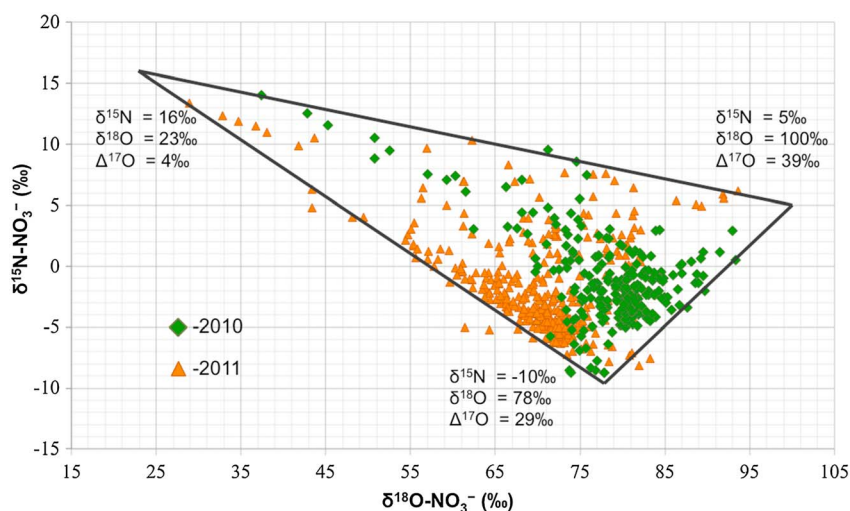
Figure 8. The relationship between $\delta^{15}N$ and $\delta^{18}O$-NO_3^- in surface snow in both 2010 and 2011. The green diamonds represent 2010 snow samples and the orange triangles represent snow samples from 2011. The samples all fall within a triangle with vertices at $\delta^{18}O = 23$‰, $\delta^{15}N = 16$‰; $\delta^{18}O = 78$‰, $\delta^{15}N = -10$‰; $\delta^{18}O = 100$‰, $\delta^{15}N = 5$‰, ($\Delta^{17}O = 4$, 29, and 39‰, respectively, not shown) each representing a distinct NO_3^- source to Summit.

4.3.2. Midlatitude NO_x

The NO_3^- source end-member with $\delta^{15}N$ of -10‰, $\Delta^{17}O$ of 29‰, and $\delta^{18}O$ of 78‰ is consistent with observations of midlatitude NO_3^-. In a typical spring, the vast majority (85%) of air transported to Summit is sourced from North America, based on 10 day, 700 hPa back trajectories [*Kahl et al.*, 1997]. This air should be influenced by a mixture of anthropogenic and natural NO_x sources that can be found in northern North America. Biomass burning should be a prominent natural NO_x source in the region [*Emmons et al.*, 2015] and NO_x from biomass burning has a $\delta^{15}N$ ranging from -7 to $+12$‰, but the value should depend on the biomass type [*Fibiger and Hastings*, 2013]. Over northern North America significant emissions are derived from burning of boreal forests that are nitrogen limited and contain a negative $\delta^{15}N$ [*Amundson et al.*, 2003], so the NO_x emitted should be closer to the low end of the above range. In addition, vehicle emissions should be important and have been measured with a $\delta^{15}N$ from -19 to $+10$‰ [*Ammann et al.*, 1999; *Heaton*, 1990; *Moore*, 1977; *Walters et al.*, 2015]. While the entire range (-19 to $+9.8$‰) has been measured in North America [*Walters et al.*, 2015], it is not clear if those direct tailpipe emissions are reflective of the NO_x undergoing long-range transport. The only roadside measurements done by *Ammann et al.* [1999] were collected passively and the study was not conducted in North America, so it is unknown how applicable that range (-4.7 to $+10$‰) may be. Coal burning for electricity generation should also be a prominent anthropogenic NO_x source in North America and the reported $\delta^{15}N$-NO_x ranges from 9 to 26‰ [*Felix et al.*, 2012; *Heaton*, 1990; *Snape et al.*, 2003]. Microbial processing of N in soils can also release NO_x and the $\delta^{15}N$ measured ranged from -47 to -28‰ during progressive release of NO_x over several days in the laboratory [*Li and Wang*, 2008]. Lightning produces NO_x with a $\delta^{15}N$ from -0.5 to $+1.4$‰ [*Hoering*, 1957]. Given this large range in NO_x emission source isotopic values, many combinations could result in a $\delta^{15}N$-NO_x close to the noted -10‰. Ideally, better-constrained source values could contribute to a more quantitative understanding of the mix of sources [*Fibiger et al.*, 2014].

Still, the 2011 season has a heavy influence of Eurasian emissions, compared with both 2010 and typical climatology for Summit (Figure 7). Thus, the end-member with $\delta^{15}N$ of -10‰, $\delta^{18}O$ of 78‰, and $\Delta^{17}O$ of 29‰, which is more important in 2011 than 2010 (Figure 8), may be indicative that the isotopes are sensitive to source region rather than directly representing the $\delta^{15}N$ of a NO_x emission source.

The oxygen isotopes fall well within the expected range for tropospheric O_3, with bulk $\delta^{18}O$ ranging from 973 to 120‰ (terminal $\delta^{18}O$ 103 to 137‰, calculated from *Michalski and Bhattacharya* [2009]) and $\Delta^{17}O$ from 20 to 27‰ (terminal $\Delta^{17}O$ 30 to 40‰) [*Johnston and Thiemens*, 1997].

4.3.3. High $\delta^{18}O$ and $\Delta^{17}O$ End-Member

The high $\delta^{18}O$ and $\Delta^{17}O$ end-member has NO_3^- with $\delta^{15}N$ of 5‰, $\Delta^{17}O$ of 39‰, and $\delta^{18}O$ of 100‰ (Figure 8). The very high $\Delta^{17}O$ and $\delta^{18}O$ are reflective of a significant influence of O_3 on the formation of NO_3^-. Based on

the ranges observed and the expectation that terminal oxygen isotopes of O_3 are involved in NO_3^- formation, either tropospheric or stratospheric O_3 could be implicated. The values observed in the snow, however, are very high compared to prior observations of $\delta^{18}O$ or $\Delta^{17}O$ of NO_3^- in the midlatitudes or other regions of the Arctic. Outside of Greenland, Arctic observations are limited, but at Alert, Nunavut, Canada, the maximum $\Delta^{17}O$-NO_3^- observed has been 35‰ and the maximum $\delta^{18}O$ 92‰ [*Morin et al.*, 2007; *Morin et al.*, 2008]. In Svalbard, the maximum $\delta^{18}O$-NO_3^- found was 81‰ [*Vega et al.*, 2015]. In the midlatitudes, the maximum observed $\delta^{18}O$ and $\Delta^{17}O$ of NO_3^- is even lower, with maximum $\Delta^{17}O$ of 30‰ and $\delta^{18}O$ of ~80‰ [*Michalski et al.*, 2012, and references therein]. This makes the observations of NO_3^- at Summit uniquely high in both $\Delta^{17}O$ and $\delta^{18}O$ for the Northern Hemisphere. So this either indicates unusual spring/summer chemistry involving only tropospheric O_3 with no participation of other oxidants (OH, HO_2, or H_2O), or the oxygen isotopes are derived from stratospheric O_3, with its higher $\Delta^{17}O$ and $\delta^{18}O$ and the possibility of involvement of other oxidants.

Stratospheric O_3 is a large fraction of the O_3 throughout the Northern Hemisphere in the springtime, and seeing that influence on NO_3^- production in the troposphere is not unexpected [*Wespes et al.*, 2012]. The $\delta^{15}N$ of stratospheric NO_3^- has never been measured directly, but has been calculated as 19 ± 3‰ from the fractionation of the reaction $N_2O + O(^1D)$, the primary source of NO in the stratosphere [*Savarino et al.*, 2007] and higher than the observed end-member value of 5‰ (Figure 8). Therefore, the complete isotopic composition raises three possibilities: (1) the NO_3^- is formed in the stratosphere and the 5‰ reflects additional fractionations in NO oxidation to NO_3^- and deposition, (2) the NO_3^- reflects tropospheric sources and chemistry but reflects only O_3 oxidation (which has not been previously reported), or (3) the NO_3^- is forming in the troposphere but shows oxidation by stratospheric O_3 that has been mixed down. In any case, the high $\delta^{18}O$, $\Delta^{17}O$ end-member shows greater influence in 2010 than 2011 (Figure 8), so that input must be different between the field seasons.

In case 1, where the NO_3^- is stratospheric in origin, there are significant differences in stratospheric chemistry between the two years. This observation fits with the Arctic ozone hole observed in 2011 [*Manney et al.*, 2011], as less stratospheric O_3 should result in lower production of NO_3^- by the stratospheric O_3 pathway. In case 2, tropospheric sources of NO_x must be oxidized by O_3 alone, which has not been observed in the middle or high latitudes of the Northern Hemisphere. Observed midlatitude $\Delta^{17}O$- and $\delta^{18}O$-NO_3^- show seasonal cycles, with highest values in winter (when O_3 chemistry should dominate) and lowest in the summer [*Michalski et al.*, 2012]. The springtime shows intermediate values. There are no observations of spring or summer NO_3^-, which has only been influenced by tropospheric O_3 and no other oxidants. While local BrO is not affecting the NO_3^- found in the snow, regional halogen chemistry could influence the NO_3^- observed [*Morin et al.*, 2007]. If only terminal atoms of O_3 are involved in NO_x oxidation, BrO should have the same isotopic influence on NO_3^- as O_3.

The third case, where the NO_3^- may be formed in the troposphere but shows influence of stratospheric O_3, would explain the unusually high $\delta^{18}O$ and $\Delta^{17}O$ while still allowing for more typical spring and summer chemistry. As explained by *Vicars and Savarino* [2014], however, photolysis of O_3, whether stratospheric or tropospheric in origin, should cause the isotopic composition to reset to local conditions. In Grenoble, France, *Vicars and Savarino* [2014] estimated this would take approximately 30 min during daylight hours. If the stratospheric O_3 were mixed into the troposphere near dusk or at night, however, this time should be extended up to several hours, particularly, if the NO_x concentrations are low. While at Summit in May and June, sunlight is constant, this is not true in the midlatitude source regions that influence Summit (Figure 7). In particular, over the remote marine boundary layer, NO_x concentrations should be very low, so the nighttime lifetime of O_3 against photolysis could allow for significant oxidation of NO_x to NO_3^-. There is no diurnal cycle in the frequency of stratospheric intrusion events [*Lefohn et al.*, 2011]. To see the influence of stratospheric O_3, both the stratosphere-troposphere exchange and the NO_x oxidation would have to occur near dusk, so this scenario would likely only happen under limited circumstances.

4.3.4. Local Anthropogenic Influence

The final NO_3^- source, with $\delta^{15}N$ of 16‰ and $\delta^{18}O$ of 23‰, has the most surprising isotopic composition. The $\delta^{18}O$, which corresponds with a $\Delta^{17}O$ of 0‰, is extraordinarily low to find in atmospherically derived NO_3^- [*Kendall et al.*, 2007; *Michalski et al.*, 2012]. This point of the triangle is filled out by NO_3^- snow samples from the isotope deviations (Figure 6), implying that this NO_3^- is formed locally at Summit. The $\delta^{15}N$ and $\delta^{18}O$ are comparable to measurements by *Proemse et al.* [2012] of NO_3^- produced in stacks of a bitumen processing facility in the tar sands of Alberta, Canada. The $PM_{2.5}$ stack emissions had a mean $\delta^{15}N$ of 16.1‰ $\pm$ 1.2‰ and
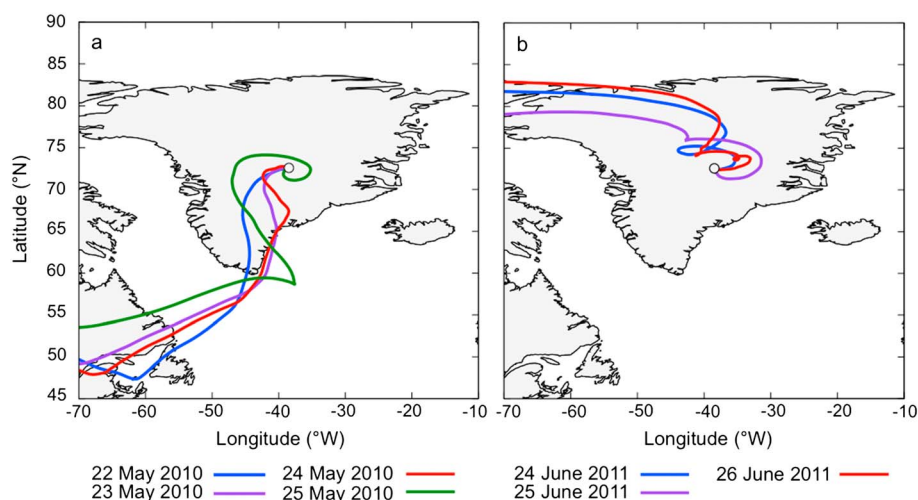
Figure 9. The pathway of air arriving at the measurement site on the days preceding, during, and after the anomalous isotope events on (a) 24 May 2010 and (b) 25 June 2011. The trajectories are the centroid locations of the particle clusters from a FLEXPART backward simulation for the period. While transport patterns are very different between the two events, they are very similar in the days surrounding each event.

$\delta^{18}O$ of 17.6‰ ± 1.8‰. Furthermore, snow samples from several shallow snow pits were sampled in an area that is typically downwind of the camp generator. All the samples showed relatively high $\delta^{15}N$ and low $\delta^{18}O$ of NO_3^-. The $\delta^{15}N$ in these snowpits ranged from 2 to 10‰, with six out of eight samples $\delta^{15}N > 6$‰. The $\delta^{18}O$ ranged from 42 to 66‰ and $\Delta^{17}O$ from 10 to 21‰. The $\delta^{18}O$-NO_3^- of 23‰ is consistent with the isotopic composition of molecular oxygen, 23.9‰ [*Barkan and Luz*, 2005], which should be the primary oxidant available in the dark generator stack.

Great efforts are made to minimize the local anthropogenic influence at Summit. It is, however, inevitable that some fossil fuel combustion occurs, particularly a diesel generator (burning Jet A-1 fuel) and several diesel-powered heavy equipment pieces used to groom the skiway and dig snow for water. Heavy equipment usage is minimized during conditions when air is carried over the station before the clean air sector (i.e., north winds) or when wind speed is minimal ($<2\,m\,s^{-1}$). The generator, however, is always operating. Prior work has shown that elemental carbon (EC) from camp activities causes concentrations 1.8–2.4 times higher at 1 km than 10 or 20 km from camp [*Hagler et al.*, 2008]. While this study focused on EC as a tracer of local emissions, it raises the expectation of similar results for other atmospheric species.

Perhaps the most confounding thing about these anomalous isotope events is the fast recovery to prior isotope values (Figure 6). This seems best explained by a physical loss of nitrate from the snow, as any chemical loss should result in fractionation that would not return to prior values in both $\delta^{15}N$-NO_3^- and $\delta^{18}O$-NO_3^-. The largest events (14 May in 2010 and 26 June in 2011) occur during very low wind speeds ($<2\,m\,s^{-1}$). The recovery in 2010 occurs after winds increase to over $2\,m\,s^{-1}$, perhaps resulting in scouring of the top layer of snow. This could remove the snow contaminated with the locally produced NO_3^- and return the NO_3^- isotopes to their prior values.

Event-based modeling of atmospheric transport to Summit also indicates that this NO_3^- is likely derived from local pollution (i.e., the generator). During the largest 2010 event, occurring on 24 May, the air is derived from south of Summit, over maritime Canada (Figure 9a). The two days prior and day following, at the same times as the event (7:00–15:00 WGDT, 9:00–17:00 UTC), show very similar origins to air during the event, despite the snow samples having very different isotopic composition. In 2011, during the largest event on 26 June, the air is all derived from north of Summit (Figure 9b). Again, the two days prior to the event (the event occurred on the last day of sampling, so the following day was omitted in 2011) show very similar air mass origins to the day of the event. The difference in air mass source between the two events that show similar isotopic composition indicates that the NO_3^- with the anomalous isotopic composition is not being transported in. Additionally, the similarity over the days before and after indicates that it is not a change in air source that is driving the radical change in NO_3^- isotopic composition. All of this indicates that the NO_3^- during the events is being driven by locally formed NO_3^-, but that NO_3^- is still not reflecting local atmospheric conditions

measured. This implies that the NO_3^- is formed under different chemical conditions than that observed over the clean air sector, likely in the generator stack.

Only while the winds are carrying station pollution directly over the sampling area is local anthropogenic NO_3^- the dominant form of NO_3^- in the snow, but it is nearly always present in the snow. With the sampling area approximately 1 km away from the main station, it is expected that there is a strong influence of local pollution during certain wind events, but the degree of influence at other times is notable, as the only samples with no influence of local pollution fall directly on the mixing line between the two higher $\delta^{18}O$ and $\Delta^{17}O$ end-members (Figure 8). In both seasons, but particularly in 2011, NO_3^- sourced from local combustion is an important portion of the NO_3^- pool in the snow.

4.3.5. Role of OH in Nitrate Production

It is surprising that NO_3^- derived from midlatitude NO_x shows no influence of OH on the oxygen isotopic composition. As shown in *Fibiger et al.* [2013], the closest fit of the linear relationship between $\Delta^{17}O$ and $\delta^{18}O$ of NO_3^- at Summit is a mixing line between O_2 ($\Delta^{17}O = 0‰$, $\delta^{18}O = 23.9‰$ [*Barkan and Luz*, 2005]) and O_3 ($\Delta^{17}O = 39‰$ and $\delta^{18}O = 100‰$). This is consistent with the end-members shown in the three-point mixing in Figure 8, with the "local anthropogenic influence" point corresponding to O_2 isotopic composition and the stratospherically influenced point fitting with the maximum O_3 $\Delta^{17}O$ and $\delta^{18}O$ presented (39‰ and 100‰, respectively). The "midlatitude" point on the three-point mixing falls along that line because it is also O_3, but with lower $\Delta^{17}O$ and $\delta^{18}O$.

In contrast, OH is expected to have a $\delta^{18}O$ between $-10‰$ and $-50‰$ (depending on fractionation from the isotopic composition of H_2O [*Michalski et al.*, 2012]) and $\Delta^{17}O$ of 0‰. These values are very far from the observed $\delta^{18}O$ of 18 to 23‰ for the lowest $\delta^{18}O$ and $\Delta^{17}O$ end-member. One possible explanation is that OH is not involved in the formation of NO_3^- in the summertime, though that seems unlikely, based on numerous laboratory, field, and modeling studies [e.g., *Donahue et al.*, 1997; *Logan et al.*, 1981; Monks, 2005; *Stroud et al.*, 2003]. Another possibility is that the assumed isotopic composition of OH is incorrect. The current predicted ranges assume either complete equilibrium with water, fractionation from H_2O or some (minimal) influence of O_3 as a source of OH [*Morin et al.*, 2007; *Michalski et al.*, 2012]. Either that assumption is wrong or the calculated fractionation of that equilibrium [*Michalski et al.*, 2012] is incorrect. Further isotopic work will be needed to determine which of these scenarios is correct.

5. Conclusions

In two May–June field seasons at Summit, Greenland, NO_3^- in the surface snow reflects long-range transported NO_3^- deposited primarily via snowfall. There is no relationship between the isotopes of NO_3^- observed in the snow and the overlying atmospheric composition. Additionally, the interannual variability in the oxygen isotopes of NO_3^- in the snow shows the opposite relationship to the oxygen isotopes of NO_3^- in the air. There are three, isotopically distinct, sources of NO_3^- to Summit. The first, with $\delta^{15}N = 5‰$, $\Delta^{17}O = 39‰$, and $\delta^{18}O = 100‰$ may indicate influence by stratospheric O_3, or may be primarily derived from North American emission sources combined with halogen-mediated oxidation chemistry or O_3 oxidation alone. Another source, with $\delta^{15}N = -10‰$, $\Delta^{17}O = 29‰$, and $\delta^{18}O = 78‰$, is most appropriately described as NO_3^- derived from midlatitude NO_x, possibly indicative of Eurasian emissions and tropospheric ozone. The final source, $\delta^{15}N = 16‰$, $\Delta^{17}O = 4‰$, and $\delta^{18}O = 23‰$, is most fittingly characterized as local anthropogenic pollution from Summit Station activities. Based on the observations, local halogen chemistry cannot explain the underestimation of $\Delta^{17}O$ in models [*Alexander et al.*, 2009; *Kunasek et al.*, 2008]. Overall, the observations indicate that local photolytic processing of NO_3^- is not important to NO_3^- preserved in the snow, as no direct relationships exist between gas phase chemistry, including local atmospheric NO_3^- and the snow NO_3^- concentrations and isotopic composition.

References

Alexander, B., M. G. Hastings, D. J. Allman, J. Dachs, J. A. Thornton, and S. A. Kunasek (2009), Quantifying atmospheric nitrate formation pathways based on a global model of the oxygen isotopic composition (delta O-17) of atmospheric nitrate, *Atmos. Chem. Phys.*, 9(14), 5043–5056.

Ammann, M., R. Siegwolf, F. Pichlmayer, M. Suter, M. Saurer, and C. Brunold (1999), Estimating the uptake of traffic-derived NO_2 from N-15 abundance in Norway spruce needles, *Oecologia*, 118(2), 124–131.

Amundson, R., A. T. Austin, E. A. G. Schuur, K. Yoo, V. Matzek, C. Kendall, A. Uebersax, D. Brenner, and W. T. Baisden (2003), Global patterns of the isotopic composition of soil and plant nitrogen, *Global Biogeochem. Cycles*, 17(1), 1031, doi:10.1029/2002GB001903.

Barkan, E., and B. Luz (2005), High precision measurements of O-17/O-16 and O-18/O-16 ratios in H_2O, *Rapid Commun. Mass Spectrom.*, 19(24), 3737–3742, doi:10.1002/rcm.2250.

Berhanu, T. A., C. Meusinger, J. Erbland, R. Jost, S. K. Bhattacharya, M. S. Johnson, and J. Savarino (2014), Laboratory study of nitrate photolysis in Antarctic snow. II. Isotopic effects and wavelength dependence, *J. Chem. Phys.*, *140*(24, 244306), doi:10.1063/1.4882899.

Blunier, T., G. L. Floch, H. W. Jacobi, and E. Quansah (2005), Isotopic view on nitrate loss in Antarctic surface snow, *Geophys. Res. Lett.*, *32*, L13501, doi:10.1029/2005GL023011.

Böhlke, J. K., S. J. Mroczkowski, and T. B. Coplen (2003), Oxygen isotopes in nitrate: New reference materials for 18O:17O:16O measurements and observations on nitrate-water equilibration, *Rapid Commun. Mass Spectrom.*, *17*(16), 1835–1846, doi:10.1002/rcm.1123.

Casciotti, K. L., D. M. Sigman, M. G. Hastings, J. K. Bohlke, and A. Hilkert (2002), Measurement of the oxygen isotopic composition of nitrate in seawater and freshwater using the denitrifier method, *Anal. Chem.*, *74*(19), 4905–4912, doi:10.1021/ac020113w.

Chen, G., et al. (2007), An assessment of the polar HOx photochemical budget based on 2003 Summit Greenland field observations, *Atmos. Environ.*, *41*(36), 7806–7820, doi:10.1016/j.atmosenv.2007.06.014.

Dibb, J. E., and M. Fahnestock (2004), Snow accumulation, surface height change, and firn densification at Summit, Greenland: Insights from 2 years of in situ observation, *J. Geophys. Res.*, *109*, D24113, doi:10.1029/2003JD004300.

Dibb, J. E., and J.-L. Jaffrezo (1997), Air-snow exchange investigations at Summit, Greenland: An overview, *J. Geophys. Res.*, *102*(C12), 26,795–26,807, doi:10.1029/96JC02303.

Dibb, J. E., R. W. Talbot, and M. H. Bergin (1994), Soluble acidic species in air and snow at Summit, Greenland, *Geophys. Res. Lett.*, *21*(15), 1627–1630, doi:10.1029/94GL01031.

Dibb, J. E., M. Arsenault, M. C. Peterson, and R. E. Honrath (2002), Fast nitrogen oxide photochemistry in Summit, Greenland snow, *Atmos. Environ.*, *36*(15–16), 2501–2511, doi:10.1016/s1352-2310(02)00130-9.

Dibb, J. E., S. I. Whitlow, and M. Arsenault (2007), Seasonal variations in the soluble ion content of snow at Summit. Greenland: Constraints from three years of daily surface snow samples, *Atmos. Environ.*, *41*(24), 5007–5019, doi:10.1016/j.atmosenv.2006.12.010.

Dibb, J. E., L. D. Ziemba, J. Luxford, and P. Beckman (2010), Bromide and other ions in the snow, firn air, and atmospheric boundary layer at Summit during GSHOX, *Atmos. Chem. Phys.*, *10*(20), 9931–9942, doi:10.5194/acp-10-9931-2010.

Donahue, N. M., M. K. Dubey, R. Mohrschladt, K. L. Demerjian, and J. G. Anderson (1997), High-pressure flow study of the reactions OH + NO$_x$ → HONO$_x$: Errors in the falloff region, *J. Geophys. Res.*, *102*(D5), 6159–6168, doi:10.1029/96JD02329.

Dorling, S. R., T. D. Davies, and C. E. Pierce (1992), Cluster analysis: A technique for estimating the synoptic meteorological controls on air and precipitation chemistry—Method and applications, *Atmos. Environ.*, *26*(14), 2575–2581, doi:10.1016/0960-1686(92)90110-7.

Emmons, L. K., et al. (2015), The POLARCAT Model Intercomparison Project (POLMIP): Overview and evaluation with observations, *Atmos. Chem. Phys.*, *15*(12), 6721–6744, doi:10.5194/acp-15-6721-2015.

Erbland, J., W. C. Vicars, J. Savarino, S. Morin, M. M. Frey, D. Frosini, E. Vince, and J. M. F. Martins (2013), Air-snow transfer of nitrate on the East Antarctic Plateau—Part 1: Isotopic evidence for a photolytically driven dynamic equilibrium in summer, *Atmos. Chem. Phys.*, *13*(13), 6403–6419, doi:10.5194/acp-13-6403-2013.

Erbland, J., J. Savarino, S. Morin, J. L. France, M. M. Frey, and M. D. King (2015), Air–snow transfer of nitrate on the East Antarctic Plateau—Part 2: An isotopic model for the interpretation of deep ice-core records, *Atmos. Chem. Phys.*, *15*(20), 12,079–12,113, doi:10.5194/acp-15-12079-2015.

Felix, J. D., E. M. Elliott, and S. L. Shaw (2012), Nitrogen isotopic composition of coal-fired power plant NO$_x$: Influence of emission controls and implications for global emission inventories, *Environ. Sci. Technol.*, *46*(6), 3528–3535, doi:10.1021/es203355v.

Fibiger, D. L., and M. G. Hastings (2013), The isotopic variablity of NO$_x$ from biomass burning, in *AGU, Fall Meeting 2013*, San Francisco, Calif.

Fibiger, D. L., M. G. Hastings, J. E. Dibb, and L. G. Huey (2013), The preservation of atmospheric nitrate in snow at Summit, Greenland, *Geophys. Res. Lett.*, *40*, 3484–3489, doi:10.1002/grl.50659.

Fibiger, D. L., M. G. Hastings, A. F. Lew, and R. E. Peltier (2014), Collection of NO and NO$_2$ for isotopic analysis of NO$_x$ emissions, *Anal. Chem.*, *86*(24), 12,115–12,121, doi:10.1021/ac502968e.

Frey, M. M., J. Savarino, S. Morin, J. Erbland, and J. M. F. Martins (2009), Photolysis imprint in the nitrate stable isotope signal in snow and atmosphere of East Antarctica and implications for reactive nitrogen cycling, *Atmos. Chem. Phys.*, *9*, 8681–8696.

Galbavy, E. S., C. Anastasio, B. Lefer, and S. Hall (2007), Light penetration in the snowpack at Summit, Greenland: Part 2 Nitrate photolysis, *Atmos. Environ.*, *41*(24), 5091–5100, doi:10.1016/j.atmosenv.2006.01.066.

Grannas, A. M., et al. (2007), An overview of snow photochemistry: Evidence, mechanisms and impacts, *Atmos. Chem. Phys.*, *7*(16), 4329–4373.

Hagler, G. S. W., M. H. Bergin, E. A. Smith, M. Town, and J. E. Dibb (2008), Local anthropogenic impact on particulate elemental carbon concentrations at Summit, Greenland, *Atmos. Chem. Phys.*, *8*(9), 2485–2491.

Hastings, M. G., E. J. Steig, and D. M. Sigman (2004), Seasonal variations in N and O isotopes of nitrate in snow at Summit, Greenland: Implications for the study of nitrate in snow and ice cores, *J. Geophys. Res.*, *109*, D20306, doi:10.1029/2004JD004991.

Hastings, M. G., J. C. Jarvis, and E. J. Steig (2009), Anthropogenic impacts on nitrogen isotopes of ice-core nitrate, *Science*, *324*(5932), 1288, doi:10.1126/science.1170510.

Heaton, T. H. E. (1990), 15 N/14 N ratios of NO$_x$ from vehicle engines and coal-fired power stations, *Tellus*, *42*, 304–307.

Hoering, T. (1957), The isotopic composition of ammonia and nitrate ion in rain, *Geochim. Cosmochim. Acta*, *12*, 97–102.

Honrath, R. E., M. C. Peterson, S. Guo, J. E. Dibb, P. B. Shepson, and B. Campbell (1999), Evidence of NO$_x$ production within or upon ice particles in the Greenland snowpack, *Geophys. Res. Lett.*, *26*(6), 695–698, doi:10.1029/1999GL900077.

Honrath, R. E., Y. Lu, M. C. Peterson, J. E. Dibb, M. A. Arsenault, N. J. Cullen, and K. Steffen (2002), Vertical fluxes of NO$_x$, HONO, and HNO$_3$ above the snowpack at Summit, Greenland, *Atmos. Environ.*, *36*(15–16), 2629–2640, doi:10.1016/s1352-2310(02)00132-2.

Jaffrezo, J.-L., and C. I. Davidson (1993), The Dye 3 gas and aerosol sampling program (DGASP): An overview, *Atmos. Environ.*, *27*(17–18), 2703–2707, doi:10.1016/0960-1686(93)90303-G.

Jarvis, J. C., M. G. Hastings, E. J. Steig, and S. A. Kunasek (2009), Isotopic ratios in gas-phase HNO$_3$ and snow nitrate at Summit, Greenland, *J. Geophys. Res.*, *114*, D17301, doi:10.1029/2009JD012134.

Johnston, J. C., and M. H. Thiemens (1997), The isotopic composition of tropospheric ozone in three environments, *J. Geophys. Res.*, *102*(D21), 25,395–25,404, doi:10.1029/97JD02075.

Kahl, J. D. W., D. A. Martinez, H. Kuhns, C. I. Davidson, J. L. Jaffrezo, and J. M. Harris (1997), Air mass trajectories to Summit, Greenland: A 44-year climatology and some episodic events, *J. Geophys. Res.*, *102*(C12), 26,861–26,875, doi:10.1029/97JC00296.

Kaiser, J., M. G. Hastings, B. Z. Houlton, T. Roeckmann, and D. M. Sigman (2007), Triple oxygen isotope analysis of nitrate using the denitrifier method and thermal decomposition of N$_2$O, *Anal. Chem.*, *79*(2), 599–607, doi:10.1021/ac061022s.

Kendall, C., E. M. Elliott, and S. D. Wankel (2007), Tracing anthropogenic inputs of nitrogen to ecosystems, in *Stable Isotopes in Ecology and Environmental Science*, edited by R. Michener and K. Lajtha, pp. 375–449, Blackwell, Oxford, U. K.

Kramer, L. J., D. Helmig, J. F. Burkhart, A. Stohl, S. Oltmans, and R. E. Honrath (2015), Seasonal variability of atmospheric nitrogen oxides and non-methane hydrocarbons at the GEO Summit station, Greenland, *Atmos. Chem. Phys.*, *15*(12), 6827–6849, doi:10.5194/acp-15-6827-2015.

Krankowsky, D., P. Lämmerzahl, K. Mauersberger, C. Janssen, B. Tuzson, and T. Röckmann (2007), Stratospheric ozone isotope fractionations derived from collected samples, *J. Geophys. Res.*, *112*, D08301, doi:10.1029/2006JD007855.

Kunasek, S. A., B. Alexander, E. J. Steig, M. G. Hastings, D. J. Gleason, and J. C. Jarvis (2008), Measurements and modeling of Delta O-17 of nitrate in snowpits from Summit, Greenland, *J. Geophys. Res.*, *113*, D24302, doi:10.1029/2008JD010103.

Lefohn, A. S., H. Wernli, D. Shadwick, S. Limbach, S. J. Oltmans, and M. Shapiro (2011), The importance of stratospheric–tropospheric transport in affecting surface ozone concentrations in the western and northern tier of the United States, *Atmos. Environ.*, *45*(28), 4845–4857, doi:10.1016/j.atmosenv.2011.06.014.

Li, D. J., and X. M. Wang (2008), Nitrogen isotopic signature of soil-released nitric oxide (NO) after fertilizer application, *Atmos. Environ.*, *42*(19), 4747–4754, doi:10.1016/j.atmosenv.2008.01.042.

Liao, J., et al. (2011a), Observations of hydroxyl and peroxy radicals and the impact of BrO at Summit, Greenland in 2007 and 2008, *Atmos. Chem. Phys.*, *11*(16), 8577–8591, doi:10.5194/acp-11-8577-2011.

Liao, J., et al. (2011b), A comparison of Arctic BrO measurements by chemical ionization mass spectrometry and long path-differential optical absorption spectroscopy, *J. Geophys. Res.*, *116*, D00R02, doi:10.1029/2010JD014788.

Liao, J., et al. (2012), Characterization of soluble bromide measurements and a case study of BrO observations during ARCTAS, *Atmos. Chem. Phys.*, *12*(3), 1327–1338, doi:10.5194/acp-12-1327-2012.

Logan, J. A., M. J. Prather, S. C. Wofsy, and M. B. McElroy (1981), Tropospheric chemistry: A global perspective, *J. Geophys. Res.*, *86*(C8), 7210–7254, doi:10.1029/JC086iC08p07210.

Manney, G. L., et al. (2011), Unprecedented Arctic ozone loss in 2011, *Nature*, *478*(7370), 469–475.

McCabe, J. R., C. S. Boxe, A. J. Colussi, M. R. Hoffmann, and M. H. Thiemens (2005), dOxygen isotopic fractionation in the photochemistry of nitrate in water and ice, *J. Geophys. Res.*, *110*, D15310, doi:10.1029/2004JD005484.

Michalski, G., and S. K. Bhattacharya (2009), The role of symmetry in the mass independent isotope effect in ozone, *Proc. Natl. Acad. Sci. U.S.A.*, *106*(14), 5493–5496, doi:10.1073/pnas.0812755106.

Michalski, G., S. K. Battacharya, and D. F. Mase (2012), Oxygen isotope dynamics of atmospheric nitrate and its precursor molecules, in *Handbook of Environmental Isotope Geochemistry*, edited by M. Baskaran, pp. 613–638, Springer, New York, doi:10.1007/978-3-642-10637-8.

Monks, P. S. (2005), Gas-phase radical chemistry in the troposphere, *Chem. Soc. Rev.*, *34*(5), 376–395, doi:10.1039/B307982C.

Moore, H. (1977), Isotopic composition of ammonia, nitrogen-dioxide and nitrate in atmosphere, *Atmos. Environ.*, *11*(12), 1239–1243, doi:10.1016/0004-6981(77)90102-0.

Morin, S., J. Savarino, S. Bekki, S. Gong, and J. W. Bottenheim (2007), Signature of Arctic surface ozone depletion events in the isotope anomaly ($\Delta^{17}O$) of atmospheric nitrate, *Atmos. Chem. Phys.*, *7*(5), 1451–1469, doi:10.5194/acp-7-1451-2007.

Morin, S., J. Savarino, M. M. Frey, N. Yan, S. Bekki, J. W. Bottenheim, and J. M. F. Martins (2008), Tracing the origin and fate of NO_x in the Arctic atmosphere using stable isotopes in nitrate, *Science*, *322*(5902), 730–732, doi:10.1126/science.1161910.

Morin, S., J. Erbland, J. Savarino, F. Domine, J. Bock, U. Friess, H. W. Jacobi, H. Sihler, and J. M. F. Martins (2012), An isotopic view on the connection between photolytic emissions of NO_x from the Arctic snowpack and its oxidation by reactive halogens, *J. Geophys. Res.*, *117*, D00R08, doi:10.1029/2011JD016618.

Neuman, J. A., et al. (2010), Bromine measurements in ozone depleted air over the Arctic Ocean, *Atmos. Chem. Phys.*, *10*(14), 6503–6514, doi:10.5194/acp-10-6503-2010.

Proemse, B. C., B. Mayer, J. C. Chow, and J. G. Watson (2012), Isotopic characterization of nitrate, ammonium and sulfate in stack PM2.5 emissions in the Athabasca Oil Sands Region, Alberta, Canada, *Atmos. Environ.*, *60*, 555–563, doi:10.1016/j.atmosenv.2012.06.046.

Rothlisberger, R., M. A. Hutterli, S. Sommer, E. W. Wolff, and R. Mulvaney (2000), Factors controlling nitrate in ice cores: Evidence from the Dome C deep ice core, *J. Geophys. Res.*, *105*(D16), 20,565–20,572, doi:10.1029/2000JD900264.

Ryerson, T. B., E. J. Williams, and F. C. Fehsenfeld (2000), An efficient photolysis system for fast-response NO_2 measurements, *J. Geophys. Res.*, *105*(D21), 26,447–26,461, doi:10.1029/2000JD900389.

Savarino, J., J. Kaiser, S. Morin, D. M. Sigman, and M. H. Thiemens (2007), Nitrogen and oxygen isotopic constraints on the origin of atmospheric nitrate in coastal Antarctica, *Atmos. Chem. Phys.*, *7*(8), 1925–1945.

Shi, G., A. M. Buffen, M. G. Hastings, C. Li, H. Ma, Y. Li, B. Sun, C. An, and S. Jiang (2015), Investigation of post-depositional processing of nitrate in East Antarctic snow: Isotopic constraints on photolytic loss, re-oxidation, and source inputs, *Atmos. Chem. Phys.*, *15*(16), 9435–9453, doi:10.5194/acp-15-9435-2015.

Sigman, D. M., K. L. Casciotti, M. Andreani, C. Barford, M. Galanter, and J. K. Bohlke (2001), A bacterial method for the nitrogen isotopic analysis of nitrate in seawater and freshwater, *Anal. Chem.*, *73*(17), 4145–4153.

Silva, S. R., C. Kendall, D. H. Wilkison, A. C. Ziegler, C. C. Y. Chang, and R. J. Avanzino (2000), A new method for collection of nitrate from fresh water and the analysis of nitrogen and oxygen isotope ratios, *J. Hydrol.*, *228*(1–2), 22–36, doi:10.1016/s0022-1694(99)00205-x.

Silvente, E., and M. Legrand (1995), A preliminary study of the air-snow relationship for nitric acid in Greenland, in *Ice Core Studies of Global Biogeochemical Cycles*, edited by R. J. Delmas, pp. 225–240, Springer, Berlin, doi:10.1007/978-3-642-51172-1_11.

Snape, C. E., C. G. Sun, A. E. Fallick, R. Irons, and J. Haskell (2003), Potential of stable nitrogen isotope ratio measurements to resolve fuel and thermal NO_x in coal combustion, *Fuel Chemist. Div. Prepr.*, *48*(1), 3–5.

Stohl, A., S. Eckhardt, C. Forster, P. James, N. Spichtinger, and P. Seibert (2002), A replacement for simple back trajectory calculations in the interpretation of atmospheric trace substance measurements, *Atmos. Environ.*, *36*(29), 4635–4648, doi:10.1016/S1352-2310(02)00416-8.

Stohl, A., C. Forster, A. Frank, P. Seibert, and G. Wotawa (2005), Technical note: The Lagrangian particle dispersion model FLEXPART version 6.2, *Atmos. Chem. Phys.*, *5*, 2461–2474.

Stroud, C., et al. (2003), Photochemistry in the arctic free troposphere: NOx budget and the role of odd nitrogen reservoir recycling, *Atmos. Environ.*, *37*(24), 3351–3364, doi:10.1016/S1352-2310(03)00353-4.

Thomas, J. L., J. Stutz, B. Lefer, L. G. Huey, K. Toyota, J. E. Dibb, and R. von Glasow (2011), Modeling chemistry in and above snow at Summit, Greenland—Part 1: Model description and results, *Atmos. Chem. Phys.*, *11*(10), 4899–4914, doi:10.5194/acp-11-4899-2011.

Thomas, J. L., J. E. Dibb, L. G. Huey, J. Liao, D. Tanner, B. Lefer, R. von Glasow, and J. Stutz (2012a), Modeling chemistry in and above snow at Summit, Greenland—Part 2: Impact of snowpack chemistry on the oxidation capacity of the boundary layer, *Atmos. Chem. Phys.*, *12*(14), 6537–6554, doi:10.5194/acp-12-6537-2012.

Thomas, J. L., J. E. Dibb, J. Stutz, R. von Glasow, S. Brooks, L. G. Huey, and B. Lefer (2012b), Overview of the 2007 and 2008 campaigns conducted as part of the Greenland Summit Halogen-HO_x Experiment (GSHOX), *Atmos. Chem. Phys.*, *12*(22), 10,833–10,839, doi:10.5194/acp-12-10833-2012.

Vega, C. P., M. P. Björkman, V. A. Pohjola, E. Isaksson, R. Pettersson, T. Martma, A. Marca, and J. Kaiser (2015), Nitrate stable isotopes in snow and ice samples from four Svalbard sites, *Polar Res.*, doi:10.3402/polar.v34.23246.

Vicars, W. C., and J. Savarino (2014), Quantitative constraints on the ^{17}O-excess (Δ^{17}O) signature of surface ozone: Ambient measurements from 50°N to 50°S using the nitrite-coated filter technique, *Geochim. Cosmochim. Acta*, *135*, 270–287, doi:10.1016/j.gca.2014.03.023.

Vicars, W. C., S. K. Bhattacharya, J. Erbland, and J. Savarino (2012), Measurement of the ^{17}O-excess (Δ^{17}O) of tropospheric ozone using a nitrite-coated filter, *Rapid Commun. Mass Spectrom.*, *26*(10), 1219–1231, doi:10.1002/rcm.6218.

Walters, W. W., S. R. Goodwin, and G. Michalski (2015), Nitrogen stable isotope composition (δ^{15}N) of vehicle-emitted NO_x, *Environ. Sci. Technol.*, *49*(4), 2278–2285, doi:10.1021/es505580v.

Wespes, C., et al. (2012), Analysis of ozone and nitric acid in spring and summer Arctic pollution using aircraft, ground-based, satellite observations and MOZART-4 model: Source attribution and partitioning, *Atmos. Chem. Phys.*, *12*(1), 237–259, doi:10.5194/acp-12-237-2012.

Wu, C., M. M. Birky, and L. G. Hepler (1963), Thermochemistry of some bromine and iodine species in aqueous solution, *J. Phys. Chem.*, *67*(6), 1202, doi:10.1021/j100800a009.

Yang, J., R. E. Honrath, M. C. Peterson, J. E. Dibb, A. L. Sumner, P. B. Shepson, M. Frey, H. W. Jacobi, A. Swanson, and N. Blake (2002), Impacts of snowpack emissions on deduced levels of OH and peroxy radicals at Summit, Greenland, *Atmos. Environ.*, *36*(15–16), 2523–2534, doi:10.1016/s1352-2310(02)00128-0.